Experiments on initial behaviour of corone generated with electrical pulses superimposed on DC Bias

tu/e
Research Report
ISSN 0167-9708
Coden: TEUEDE

Eindhoven
University of Technology
Netherlands

Faculty of Electrical Engineering

Experiments on Initial Behaviour of Corona Generated with Electrical Pulses Superimposed on DC Bias

by
R.P. Dahiya
E.M. van Veldhuizen
W.R. Rutgers
L.H.Th. Rietjens

EUT Report 89-E-226
ISBN 90-6144-226-5

October 1989

Eindhoven University of Technology Research Reports

EINDHOVEN UNIVERSITY OF TECHNOLOGY

Faculty of Electrical Engineering
Eindhoven The Netherlands

ISSN 0167- 9708

Coden: TEUEDE

EXPERIMENTS ON INITIAL BEHAVIOUR OF CORONA GENERATED WITH ELECTRICAL PULSES SUPERIMPOSED ON DC BIAS

by

R.P. Dahiya
E.M. van Veldhuizen
W.R. Rutgers
L.H.Th Rietjens

EUT Report 89-E-226
ISBN 90-6144-226-5

Eindhoven
October 1989

CIP-GEGEVENS KONINKLIJKE BIBLIOTHEEK, DEN HAAG

Experiments

Experiments on initial behaviour of corona generated with electrical pulses superimposed on dc bias / by R.P. Dahiya, E.M. van Veldhuizen, W.R. Rutgers, L.H.Th. Rietjens. - Eindhoven: Eindhoven University of Technology, Faculty of Electrical Engineering. - Fig., tab. - (EUT report, ISSN 0167-9708; 89-E-226)
Met lit. opg., reg.
ISBN 90-6144-226-5
SISO 661.52 UDC 621.3.015.532 NUGI 832
Trefw.: corona-ontladingen.

ABSTRACT

In the first part of this paper the pulsed positive corona discharges in air at atmospheric pressure have been investigated. The corona has been produced in a wire-cylinder geometry by superimposing fast rising (4 μs rise time) voltage pulses of positive polarity on a dc bias. The peak pulse voltage is varied between 2.5 kV to 46 kV while the dc bias is controlled indepedently between zero to well above the corona inception. The light emission measurements show the pulsed nature of the corona created by fast electrical pulses. The light intensity is orders of magnitude higher in comparison to that from dc glow corona. The time delay between the start of the electrical pulse and the light emission decreases with the total applied voltage and is independent of the ratio of dc bias to pulse voltage. Two discharge regimes can be distinguished: When the total voltage is just above the corona inception voltage (approx. 18 kV) several light peaks with large jitter in time are observed. Beyond 26 kV two well defined, large light peaks, as expected from streamer formation, with no appreciable time delay are measured. In this discharge regime an electric current of approximately 1 Ampere flows through the pulsed corona discharge.

In the second part of this paper the initial development of a pulsed negative corona in a cylindrical configuration has been experimentally investigated. The corona has been produced in air by superimposing negative voltage pulses on a steady dc bias. Two types of pulses have been used; most of the experiments are performed with 3.5 μs rise time pulses except for one series of experiments for which faster -26.4 kV voltage pulses having a rise time of 0.6 μs are superimposed on the dc bias. The optical emission from the corona has been detected by a photomultiplier. In the corona inception region optical signal appears after a considerable time delay from the starting of the voltage pulse. This time delay decreases sharply at higher voltages. But in the absence of the dc bias the corona is initiated sometime even after time delays of more than 50 μs which suddenly switch over to small time scales of a few microsecond without any change in the experimental parameters. For voltages near the inception many light peaks are observed bunched together and at higher voltages distinct light peaks of much higher intensity are emitted which can be attributed to the formation of space charge waves. In the case of the faster rise time, delay and the variation in the delay become significantly lower, in other words the emission becomes more well defined in time. The amplitude of the light signal grows to a maximum and then decreases as the wire potential is raised, the decrease being gentle for the case of the faster electrical pulses.

Dahiya, R.P.+ and E.M. van Veldhuizen§, W.R. Rutgers*,
L.H.Th. Rietjens§
EXPERIMENTS ON INITIAL BEHAVIOUR OF CORONA GENERATED WITH ELECTRICAL PULSES SUPERIMPOSED ON DC BIAS.
Faculty of Electrical Engineering, Eindhoven University of Technology, The Netherlands, 1989.
EUT Report 89-E-226

+) Present address: Indian Institute of Technology, New Delhi, India

§) Faculty of Electrical Engineering, Eindhoven University of Technology, P.O. Box 513, 5600 MB Eindhoven, The Netherlands

*) Permanent address: N.V. KEMA Laboratories, Utrechtseweg 310, 6812 AR Arnhem, The Netherlands

Contents

Part I. Positive corona

1. Introduction

The acidic compounds exhausted along with the flue gases are responsible for acid rain. These acidic pollutants can be removed by generating appropriate pulsed positive corona discharge in the flue gases before exhausting them to atmosphere.

When a high voltage is applied to a wire fixed along the axis of a grounded air filled cylinder, corona is formed around the stressed electrode where locally the field exceeds breakdown. The corona is initiated by free electrons which ionize the gas and build up avalanches under the influence of the electrical field. Further ionization growth due to the space charge field and secondary electrons produced by photoionization leads to a current conducting path which is called a streamer. After the streamer mechanism was first suggested by Raether (1939) and Loeb and Meek (1940), formation and propagation of streamers have been investigated by several other workers (Gallimberti 1972, Kline 1974, Chalmers et al. 1972, Dhali and Williams 1987, Dhali and Pal 1988, Allen and Boutlendj 1988, Phelps and Griffiths 1976).

In large air gaps a positive impulse is known to give a spark after a finite time (Gallimberti 1979). The Schlieren technique used by Domens et al. (1988) gives information about the prebreakdown phase of long sparks. McAllister et al. (1979) have performed experiments in small air gaps to understand the inception of the positive corona discharge under the application of d.c.field. They have observed multiple avalanche development preceding the corona onset. The number of electrons at the head of primary avalanche has been taken into account by Salama et al. (1976) to evaluate the corona inception probability for a positive point to plane gap. A field dependent critical volume, where the triggering electron must exist to initiate the corona, is shown to be responsible for the statistical probability of corona initiation. Once sufficient charge is built up in avalanche it may give rise to a streamer. Two dimensional computer simulations of Dhali et al. (1987, 1988) support this streamer criterion.

The high electrical field at the positively charged head of the streamers heats electrons upto several electron volt (Spyrou et al.1989). These energetic electrons can dissociate stable molecules to

form radicals (Clements et al. 1986, Mizuno et al. 1986, Masuda and Nakao 1986, Civitano et al. 1988) which makes such a violent corona a potential candidate for 'plasma catalysis'. An important application of this process can be the removal of NOx and SO2 from flue gases. If corona is produced in flue gases by superimposing a fast rising electrical pulses on a dc bias the efficiency of removing the pollutants is enhanced. Under these conditions the ionic space charge left behind by the pulsed corona can be cleared by the dc voltage during the interpulse period.

So far the difference between corona in air and flue gas is not quite clear. A comparison between the transport coefficients of the flue gas and air has been made by Gallimberti (1988). The electron drift velocity, mean energy and ionization coefficient are shown not to change significantly by the different gas composition but the attachment coefficient is found to be greater in flue gas at high electric fields. Recent experiments made at KEMA (Verhaart 1989) confirm the small difference in drift velocity, effective ionization rate and also in attachment coefficient. Differences in (pulsed) discharge currents are attributed to detachment and conversion processes due to water vapour. Moreover, the initial behaviour of corona in the onset region is not well understood even for air when pulse voltage is superimposed on dc bias. It is, therefore, desirable to make experimental investigations on the formation of such a corona in air and in flue gas so that a working regime can be defined for practical applications.

Keeping in view the recent interest for practical applications we have studied the development of positive corona in air with and without dc bias. The light signal emitted from the corona is used to evaluate the time delay in corona inception by varying the dc bias from zero to more than inception voltages. Two different discharge regimes of pulsed corona have been observed.

2. Experimental set up

We have used a coaxial configuration to produce corona in air. The corona set up and electrical circuit used for the present experiments are shown in figure 1. High voltage pulses superimposed on dc bias are applied to a 1 mm diameter and 80 cm long wire fixed concentrically

with 20 cm diameter stainless steel cylinder. The cylinder is kept in vertical position resting at one of its faces placed on an insulating platform. The wire is hung from the top insulated end of the cylinder. A weight attached at the bottom of the wire keeps it tightly stretched. The cylinder is grounded via a 4.7 kΩ resistor.

Provision is made in the upper insulating flange to mount an optical fibre having a lens in front of it. With such an arrangement the lens focusses the light emitted from the cylindrical volume marked in the figure, on the optical fibre. The light then travels through a 100 m long fibre so that the light recording system is kept outside the shielded high voltage laboratory to prevent perturbation in the signal by the electromagnetic pulses. The other end of the fibre is coupled to a photomultiplier via a lens. The signal from the photomultiplier is digitized with a Tektronixs 7D20 digitizer and stored in the memory of a Tektronix oscilloscope 7603. The trigger signal for the oscilloscope is taken from the spark gap. Eventually the trace from the oscilloscope is transferred to a computer for further processing.

High voltage positive pulses are generated using the electrical circuit shown in figure 1 (Kloth, 1987). When the spark gap is triggered a positive pulse appears on the wire electrode. A variable positive dc bias is also applied to the wire. The crest voltage of the pulse can be varied by changing the negative power supply voltage. The pulse voltage is measured by a differentiating probe and a resistive potential divider is used for measuring the dc bias. The probe to measure the high voltage pulse is a differentiating sensor formed by a small capacitive electrode in series with 50 Ω resistor to ground. A terminated coaxial cable connecting the sensor to a wide band integrator serves as the 50 Ω resistor. This concept, with cable termination and integrator housed in a special cabinet allows good EMC qualities in high interference surroundings (van Heesch, 1987). Inside the cabinet with open frontend, the signal is digitized and stored on floppy disk using a Nicolet 4094 C oscilloscope.

The DC corona current voltage characteristic is measured by a 4.7 kΩ grounding resistor. The pulse rise time can be varied by changing the 10 kΩ resistor in series with the spark gap. For the present experiments we have used a 10 kΩ resistor, which gives a rise time of

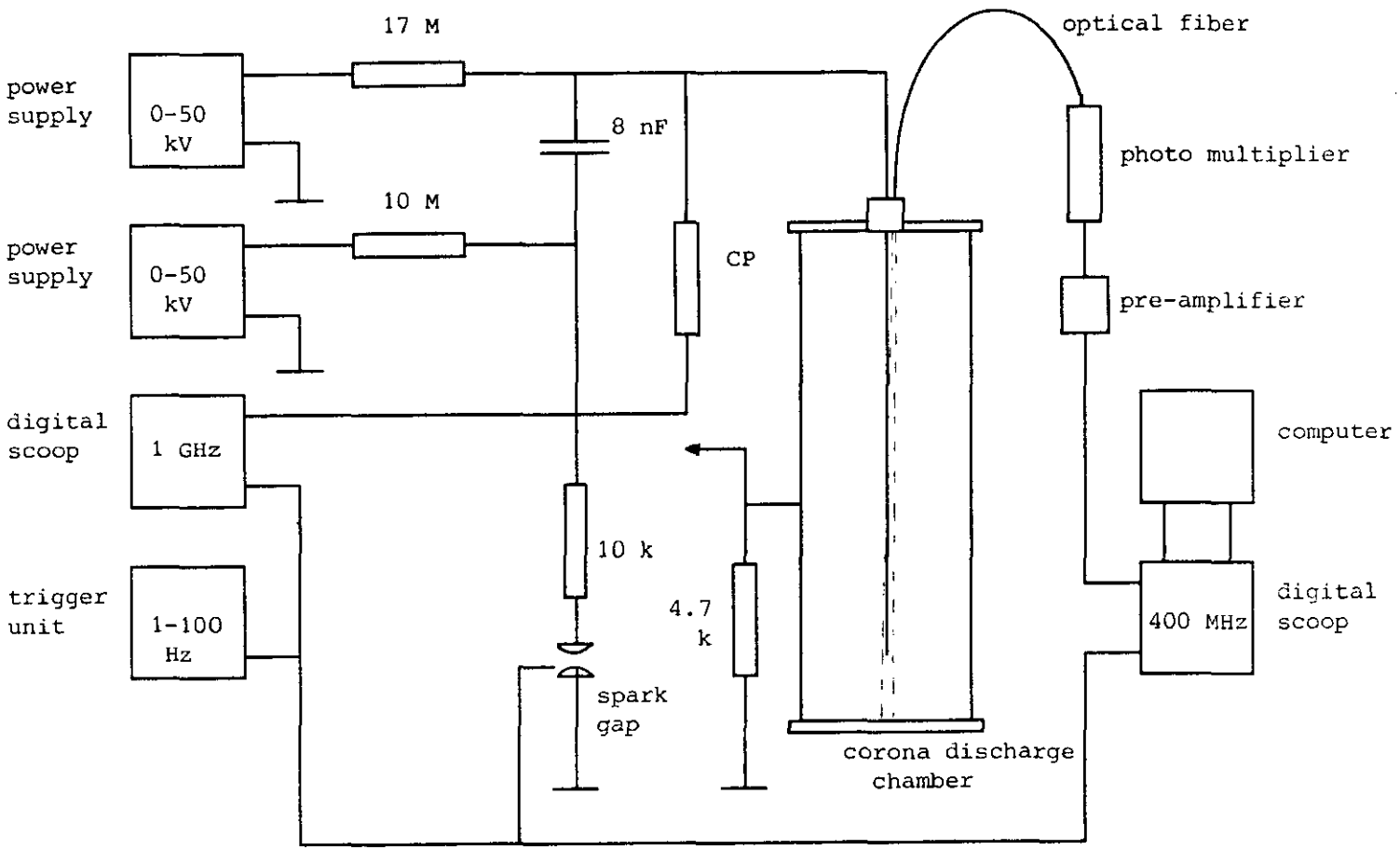

CP: capacitive probe

Figure 1. Block diagram of the experimental set up. Facility made available by the High Voltage Laboratory of the University.

nearly 4 μs. The pulserise time is independent of its crest value. A typical pulse waveform is shown in figure 2. Obviously the spark gap setting has to be changed while covering as wide a range as 2.5 kV to 46 kV for the pulsevoltage. A small flow of air around the trigger electrode of the sparkgap helps to stabilize the pulse over a wider range. The pulse repetition rate can be varied but we have used 5 pulses per second for the present experiments. Two photomultipliers have been used for the detection of the light emission. The first is an EMI 9635QA with a 10 kΩ load resistor, a 100 MHz amplifier and a comparator built into its socket. This gives single photon pulses of several volts with a rise time of 10 ns. It can be used at very low light levels. But when photons start to coincide the electronics saturate. Then we use another photomultiplier EMI 9896 QB, with a 1 kΩ load resistor and an impedance transformer having an output impedance of 50 Ω. In this situation the amplitude of the signal goes up when photons merge into one another. At low light level single pulses of 5 to 20 mV can still be recognized if 1500 V is applied across the dynodes of the photomultiplier tube. For high intensity optical pulses the power supply voltage is turned down to 1000 V which reduces the sensitivity of the photomultiplier by a factor of 10.

3. Results and Discussion

The experiments have been performed in air at ambient temperature andatmospheric pressure. The temperature inside the laboratory has been 21 °C on average. The cylinder is closed but is not air tight.

3.1. dc corona characteristics

For dc corona the time averaged current is compared with the photon yield from the corona. As shown in figure 3a the number of photons follows the current rise very well. This is expected since the photon emission and the current flow depend on the level of ionization which scales up with the applied voltage after the corona onset. Careful current measurements in the corona onset region have shown almost linear current rise right from 15.5 kV onwards. It is clear from figure 3b that a transition occurs at 18.5 kV in the current characteristic. Since the dark current in our photon counting system had a finite value we could not resolve significantly the photon yield from the corona

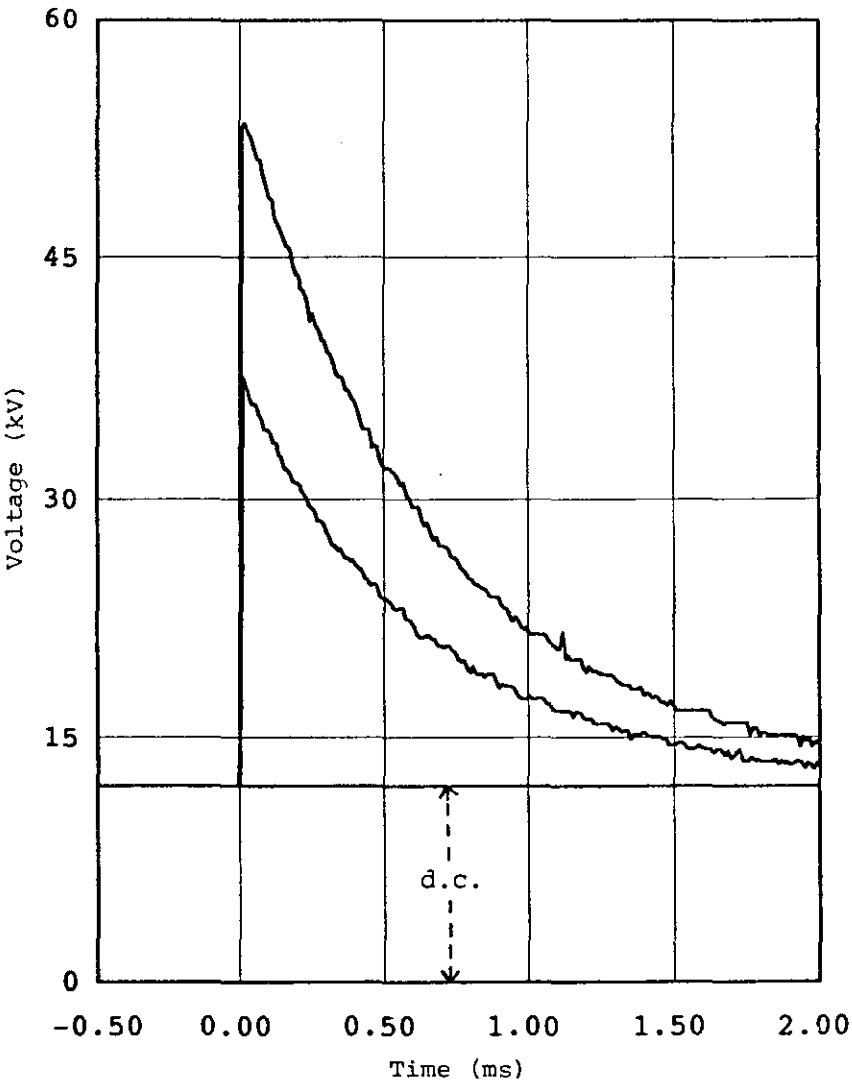

Figure 2. Two typical electrical pulses superimposed on 12 kV dc bias.

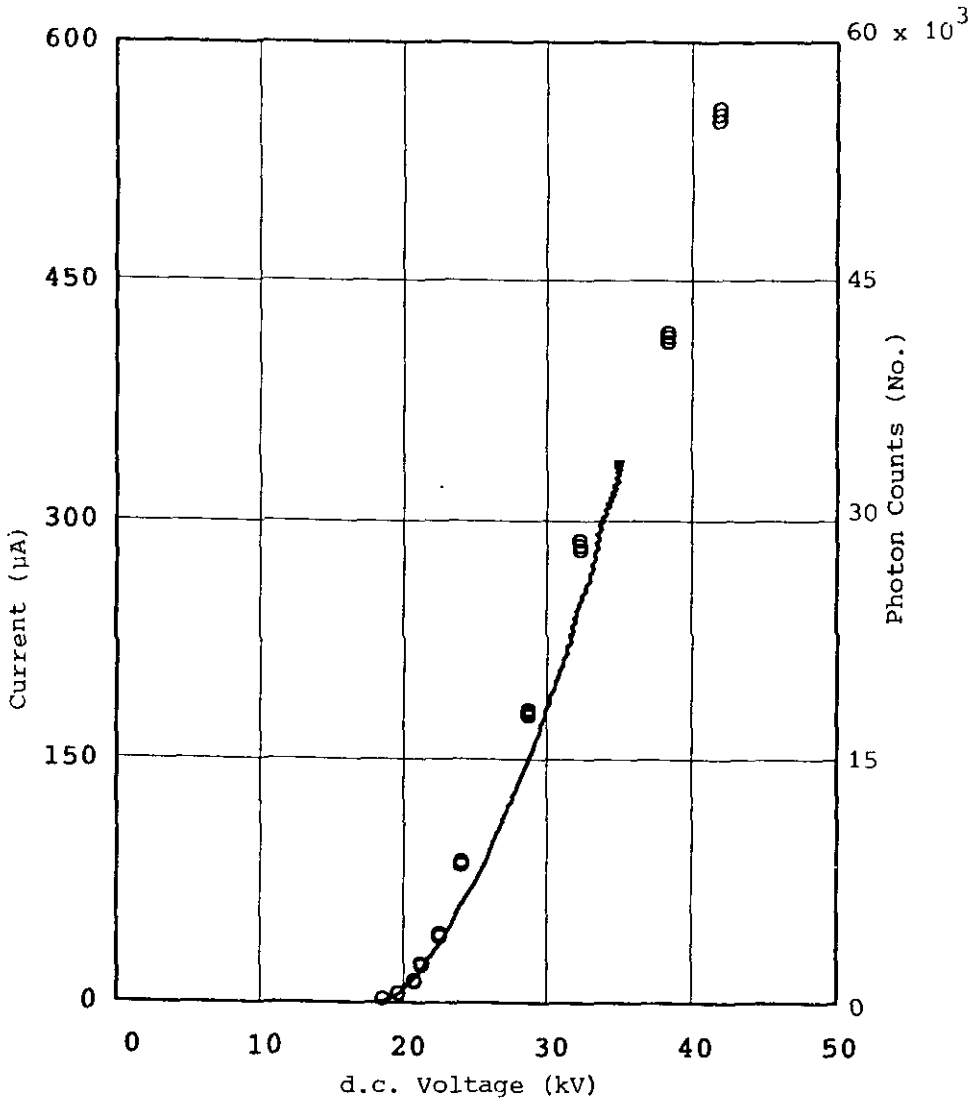

Figure 3(a). Current-voltage characteristic and photon counts (o) of dc corona.

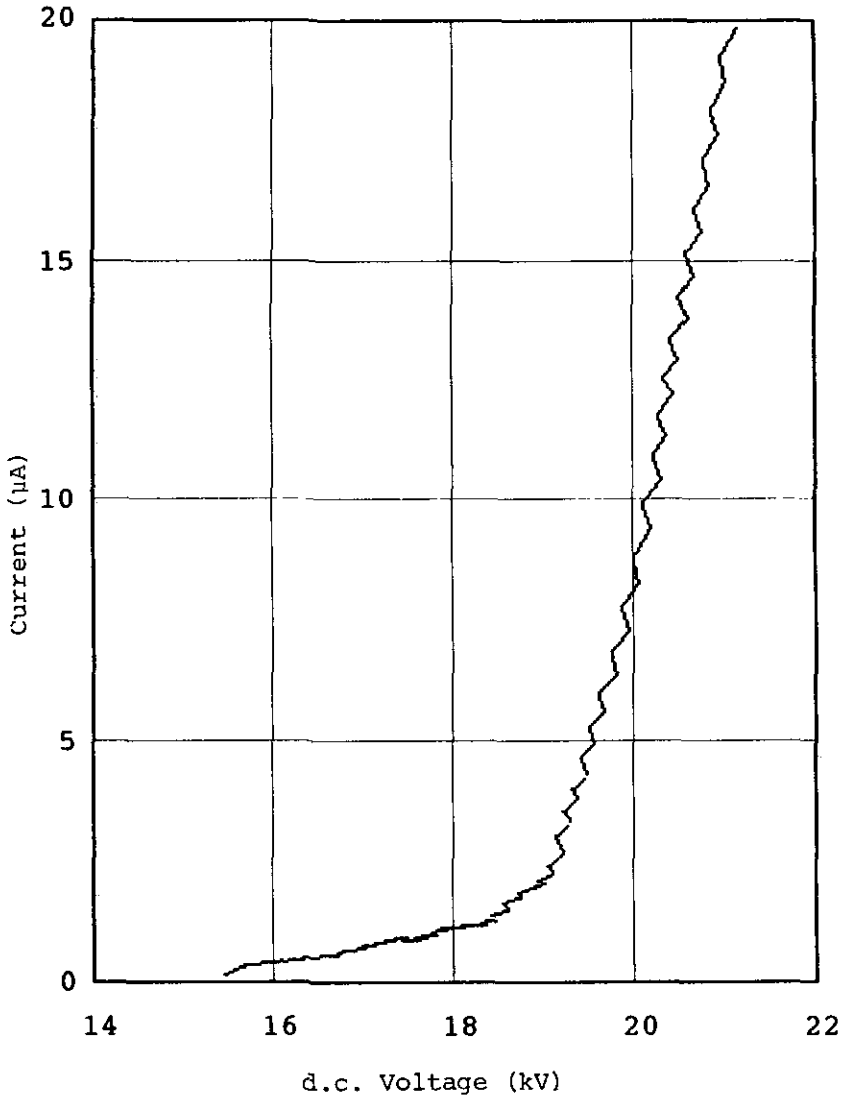

Figure 3(b). Transition in current voltage characteristic of *dc corona in the onset region.*

below 18.4 kV applied to the wire.

3.2. Pulsed corona

In case of pulsed corona we have superimposed electrical pulses of different values on variable dc bias and also used pulses without any bias. The various combinations of voltages used are given in Table 1. Since the light emission from the pulsed corona is several orders of magnitude higher than that from dc glow, we had to use the lower gain photomultiplier in order to avoid saturation. With the minimum possible setting of the spark gap we could generate 2.5 kV electrical pulses and started our measurements by raising dc bias from 18.2 kV beyond which we observed a detectable light signal. The electrical pulse voltage selection is made in such a manner that the 2.5 and 15.6 kV pulses do not initiate corona on their own but 26.0 kV pulses, even without dc bias, produce corona themselves.

For all our subsequent measurements reported in this paper the delay refers to the time lapsed between the triggering of the spark gap and the appearance of the light signal; in other words reference for time is the trigger time of the spark gap when the electrical pulse is initiated. The light emission integrated along the corona wire (emitted from the volume marked in figure 1) recorded for different electrical conditions is shown in figures 4 to 7. It is worth mentioning that even for as low a pulse voltage as 2.5 kV the light output from the pulsed corona is much higher than that from dc glow. In case of 2.5 kV pulse, shown in figure 4, we could detect optical signal at a minimum total voltage of 20.7 kV applied to the wire. Under these conditions the first optical signal peak appears after a delay ranging between 5.7 - 7.7 μs. Several distinct light peaks are observed within 2 μs from the first pulse. These peaks bunch together when the dc bias is increased till 19.9 kV (figure 4b) but thereafter again separate light peaks are observed at higher voltages and they do not merge into one another. Similarly for 15.6 kV pulses, light emission is observed at nearly the same minimum voltage. Now, as is evident from figure 5, there are signals from primary corona and secondary corona (Dawson 1965) with intervening dark periods (Marode 1975, Gallimberti 1979), for 17.0 kV and higher dc voltages (figures 5c,d). The time delay is progressively reduced at higher corona voltages.

The situation for 26.0 kV pulse is different from the ones discussed

Table I.1 Combinations of positive electrical pulses and dc bias

S.No.	Electrical Pulse			DC Bias
	crest voltage kV	rise time μs	half width μs	kV
1	2.5	3.0	---	18.2 to 43.9
2	15.6	4.0	500	5.4 to 37.4
3	26.0	4.0	500	10.5 to 31.7
4	20 to 46.2	4.0	500	0

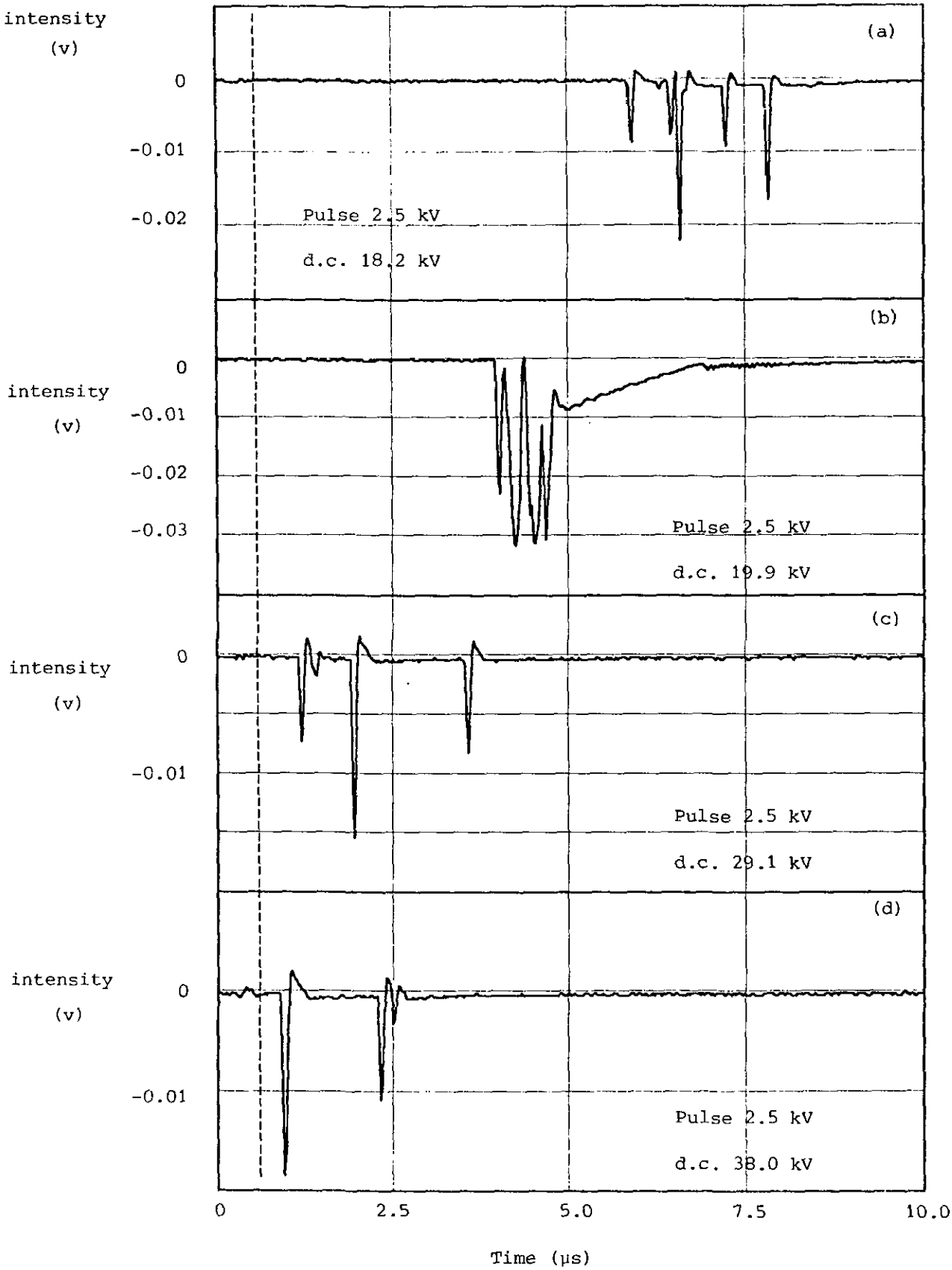

Figure 4. Optical signal emitted from positive corona generated with 2.5 kV pulse superimposed on dc bias. The bias used is marked on the respective figures.

earlier. This pulse itself can initiate corona after crossing the inception voltage. It is interesting to note from figure 6 that there are no multiple peaks of the type observed for 2.5 and 15.6 kV pulses. For all the voltages there is a main light peak corresponding to primary corona followed by smaller (in amplitude) peaks for secondary corona. If the total voltage applied to the wire is now 56 kV, and it is at this voltage that spark over occurs between the wire and the cylinder. Hence figure 6d shows the light emitted by the corona (first two peaks) as usual and, after a lapse of 7 μs, a larger optical signal is recorded due to the spark over. The change in scale of the ordinate may be noted for this case.

The observations of figure 4 to 6 suggest formation of avalanches (McAllister et al. 1979) for 2.5 and 15.6 kV pulses in the onset region. For higher voltages the discharge can take the form of a number of branched streamers whose starting points are discrete and distributed over the highly stressed electrode (Gallimberti 1972, 1988). The strong first peaks are called streamers from now on. The 26.0 kV pulses, however, always give rise to streamer formation having more well defined corona behaviour. For this case the primary streamer is followed by a less intense secondary streamer with intervening dark period (Gallimberti 1979).

When the measurements are made by applying electrical pulses only, the light signal observed from ≅20 kV onwards shows avalanche type characteristics upto 25 kV and thereafter it has primary and secondary corona peaks. Figure 7 shows the development of such a corona in the absence of the dc bias. As before, delay in corona initiation is decreased with the increase of the pulse voltage.

The statistical behaviour of corona inception is well known (Salama 1976, Gallimberti 1979). For corona inception to occur,a triggering electron should exist in a "cylindrical shell" surrounding the wire electrode, where the electric field is high enough to produce effective ionization and lead to the formation of an avalanche of critical size. The probability of having the triggering electron in the cylindrical shell gives a statistical behaviour. When the wire voltage is increased, the volume of the cylindrical shell also increases. We have measured jitter in time for emission of the light signal from the corona arising due to its statistical behaviour. The envelop made by

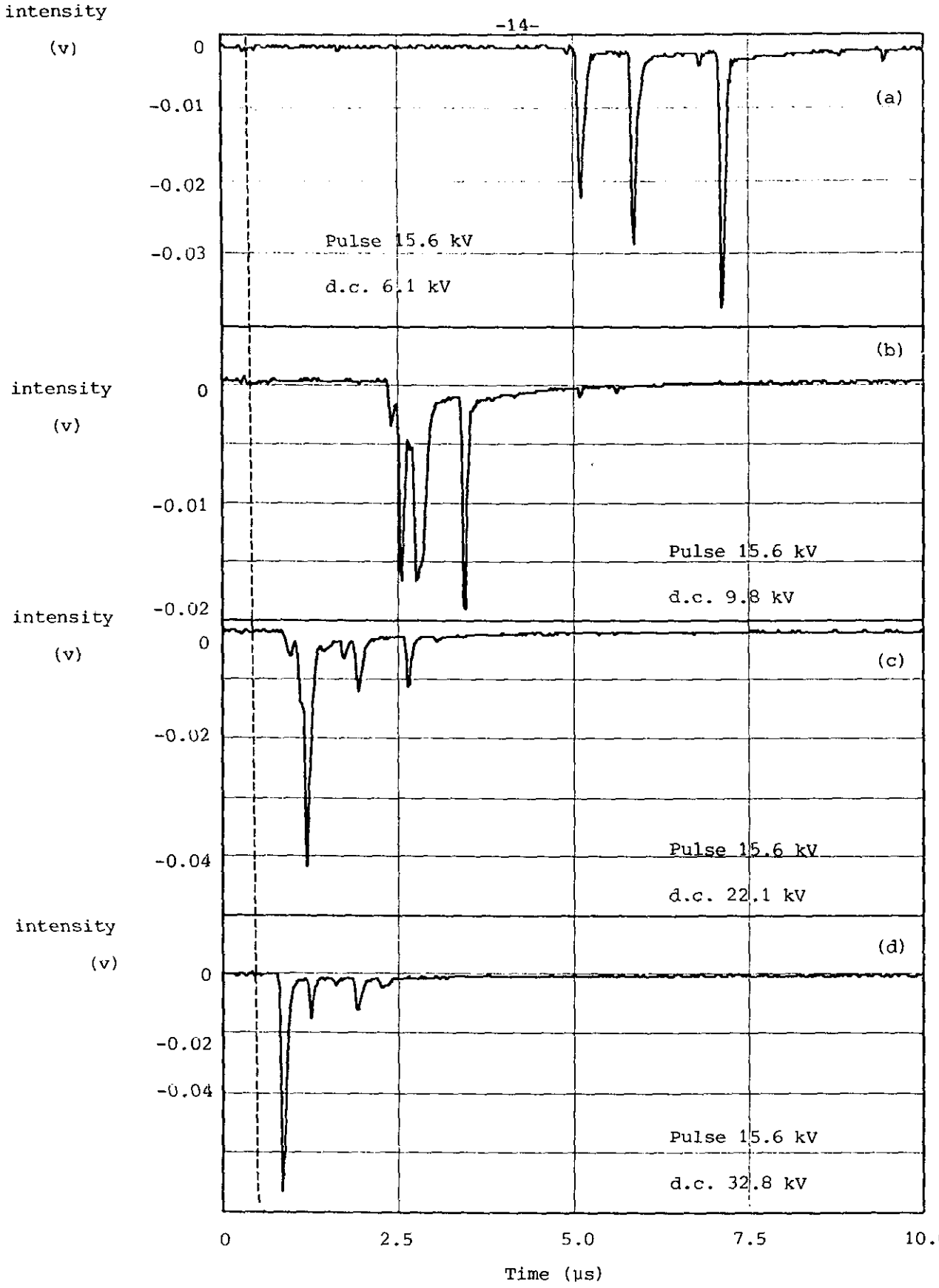

Figure 5. Optical signal emitted from corona generated with 15.6 kV pulse superimposed on dc bias. The bias used is marked on the respective figures.

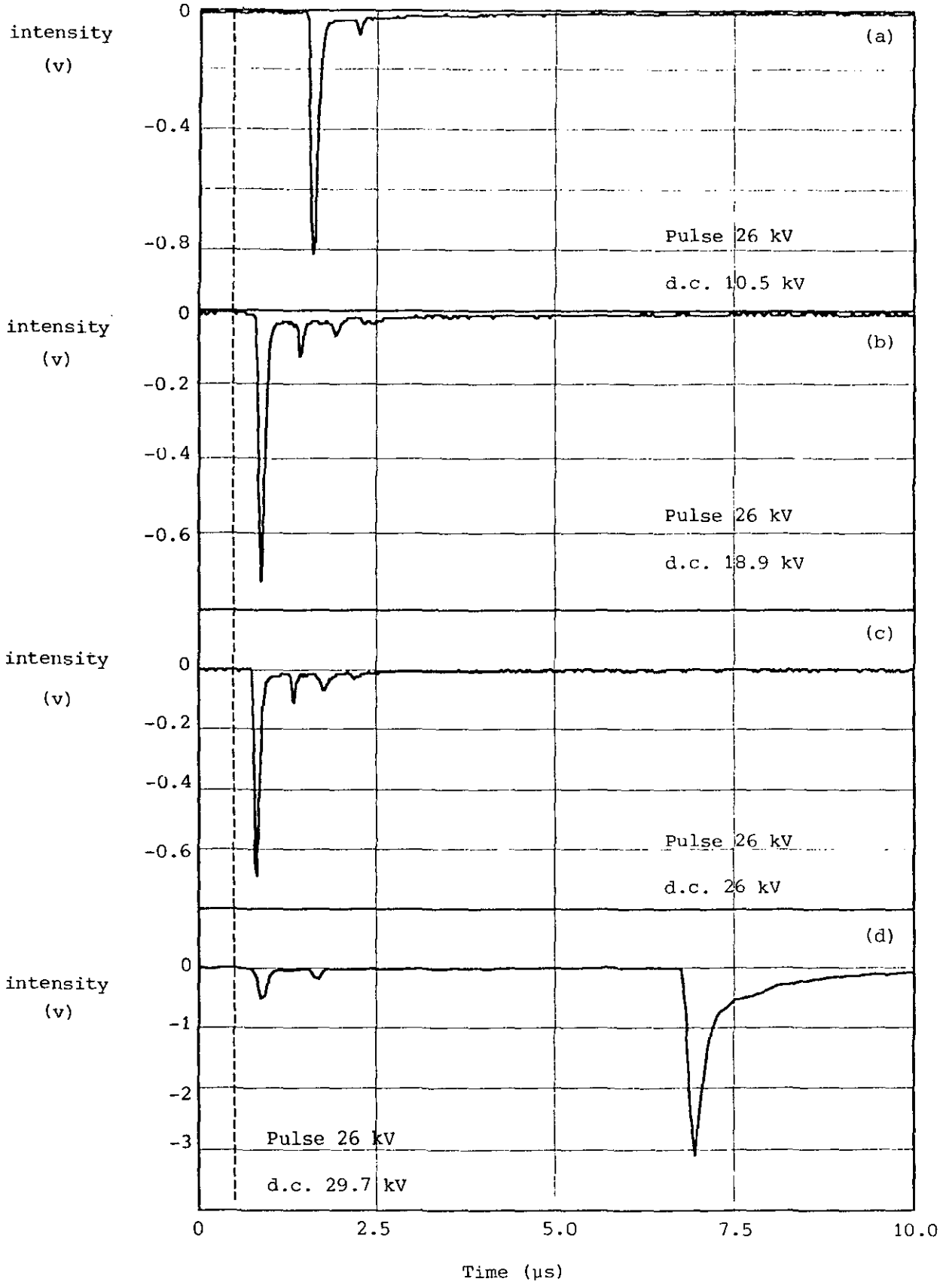

Figure 6. Optical signal emitted from corona generated with 26.0 kV pulse superimposed on dc bias. The bias used is marked on the respective figures. In (d) light peak corresponding to breakdown between the wire and cylinder appears at 7 μs.

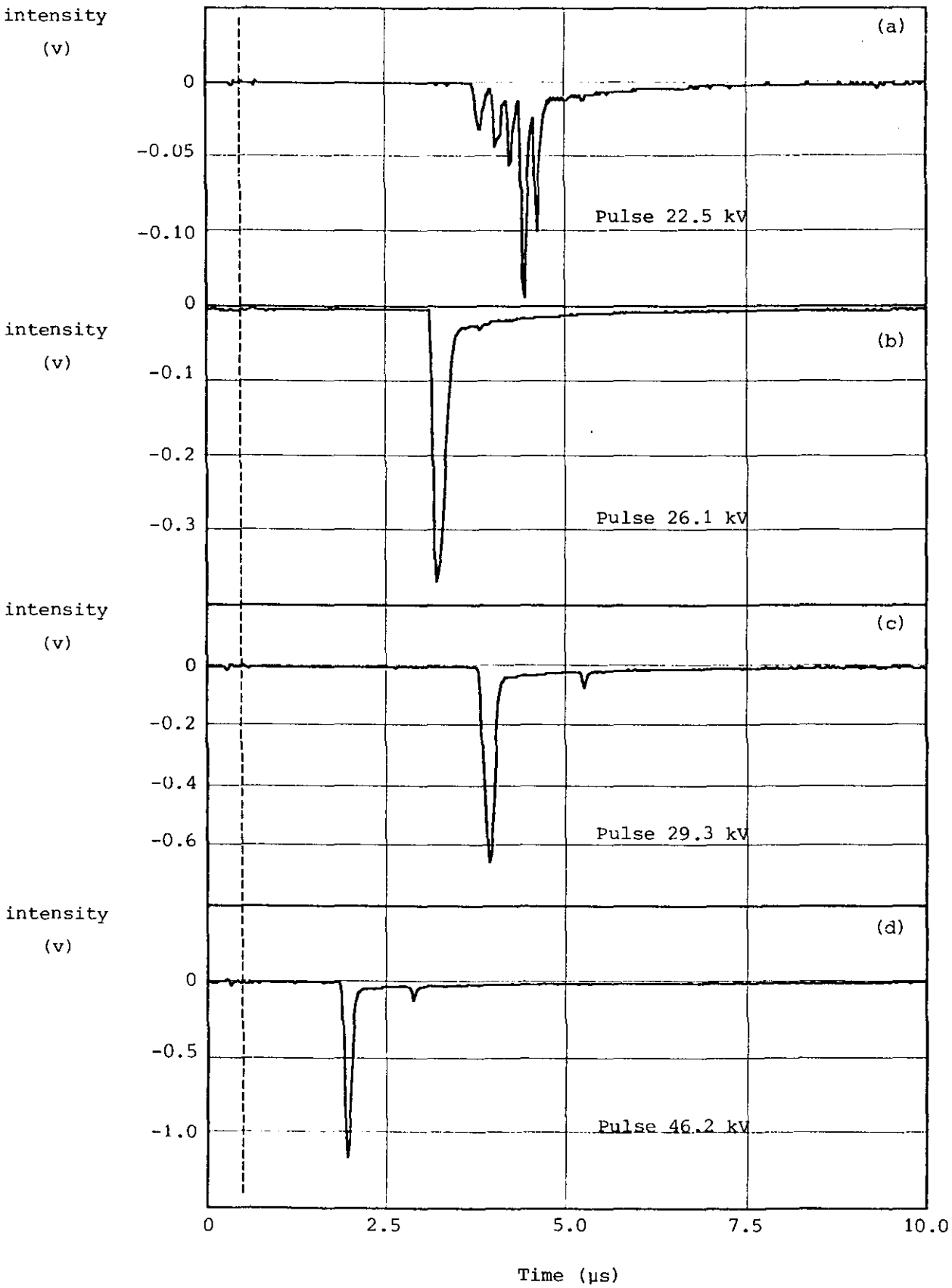

Figure 7. Optical signal emitted from corona generated with electrical pulses only. Crest voltage of pulses are marked on the respective figures.

capturing the optical signal from about 300 different electrical shots on the same channel, shown in figure 8 and 9, gives a good estimate of the fluctuation in time for corona initation. As expected, the delay as well as jitter in time become smaller at higher voltages for the primary streamer. From figure 8d we can see that this jitter is less than 100 ns. For the secondary streamer the jitter remains approximately 2 μs.

As shown earlier, there is a delay between the application of voltage on the wire and emission of light from the corona. We have measured time delay of first light peak for various combinations of pulse and dc voltages mentioned in Table I.1. The half width of the light signal peaks is approximately 75 ns: The time delay is plotted in figure 10. For 2.5, 15.6 and 26.0 kV pulses, the abscissa of the figure gives the value of dc bias but for pulses only (case 4 in Table I.1) it should be read as the crest value of the electrical pulses. All the curves tend to approach to a minimum (≈ 0.5 μs) at higher voltages. As a matter of fact this is approximately the transit time of the light signal in 100m long optical fibre. Therefore, the delay in corona initiation is almost negligible once we exceed a certain voltage. The voltages on the wire due to pulses, applied in the pulse only mode, are shown in figure 11. They have a small dip in their rising part. This corresponds in time to the emission of the light signals. The drop in electrical pulse is due to the high current of the streamers. The current giving rise to the dip of about 2 kV observed in the voltage can be estimated from CdV/dt, where C is the capacitance of the corona set-up. In the present case C is nearly 50 pF and dt, inferred from the width of the optical pulses, is approximately 75 ns. Therefore ≈1 ampere current is flowing when the streamers are formed. When the streamer propagation stops the gas around the wire is filled with positive space charge. Since the space charge reduces the applied electric field and cannot drift away within tens of microseconds, no strong second bunch of streamers is formed in spite of the still rising voltage on the wire. The light peaks are observed at a certain voltage but afterwards, even at higher crest voltage, no further light peak has been detected except for a small secondary corona signal (see figure 6).

When figure 10 is replotted by taking total voltage on the wire (pulse plus dc) as abscissa we get figure 12. Different curves for fixed pulse voltages merge into a single curve. Apparantly the pulse only curve

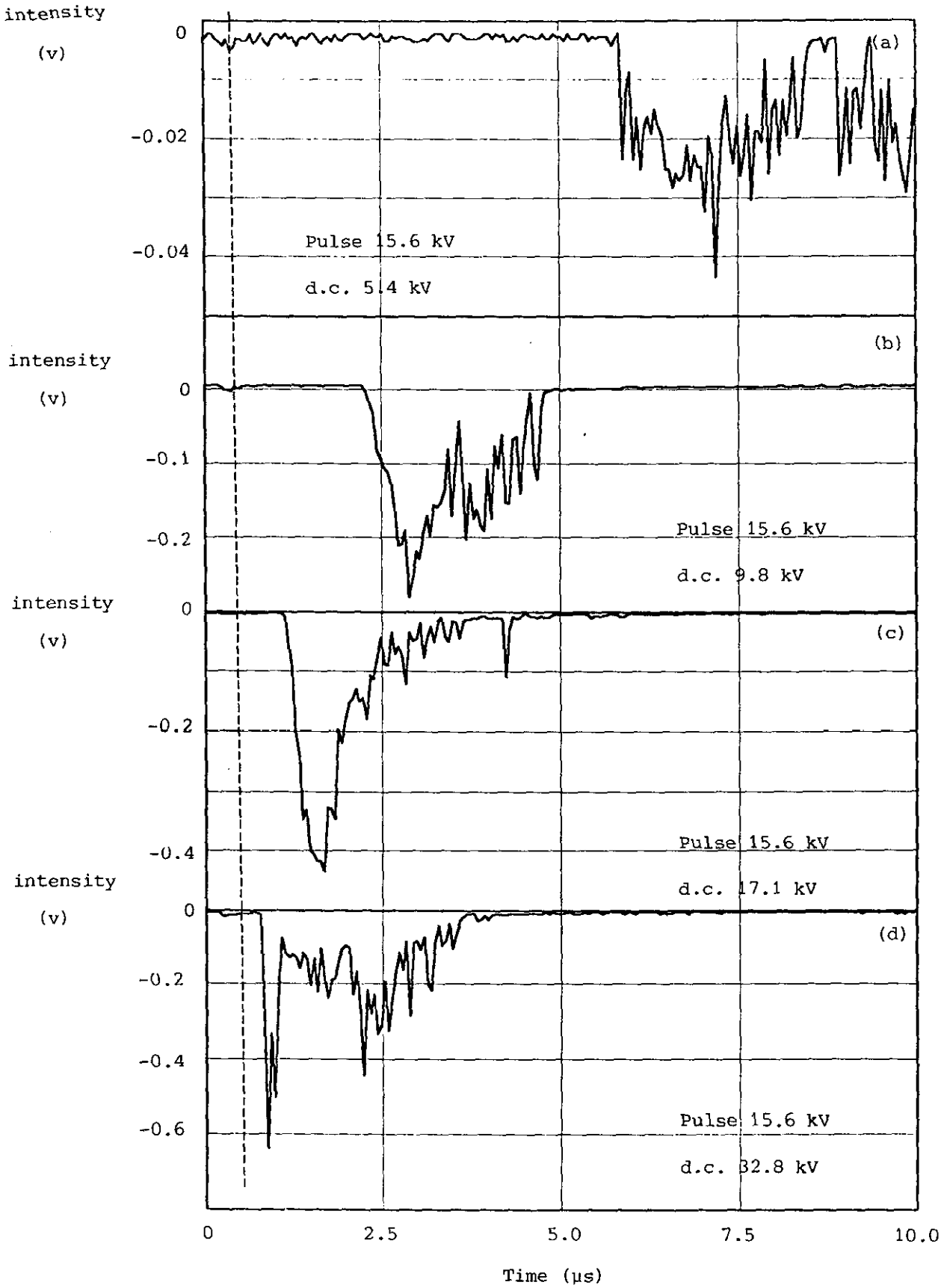

Figure 8. Envelop of light peaks emitted from corona for 300 electrical pulses of 15.6 kV each superimposed on dc bias marked on respective figures.

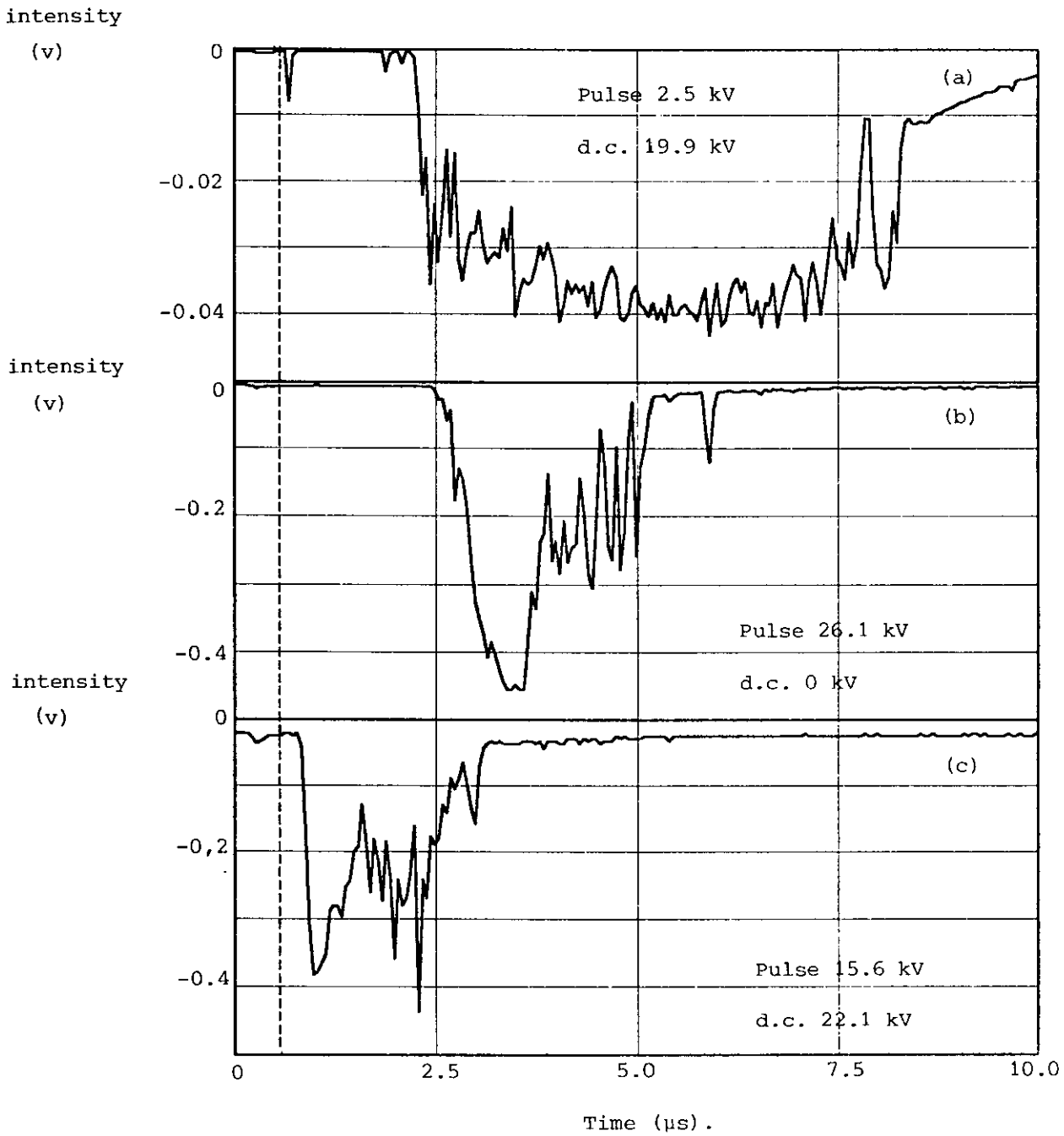

Figure 9. Envelop of light peaks emitted from corona for 300 electrical pulses. Crest voltage of pulse and dc bias are marked on the respective figures.

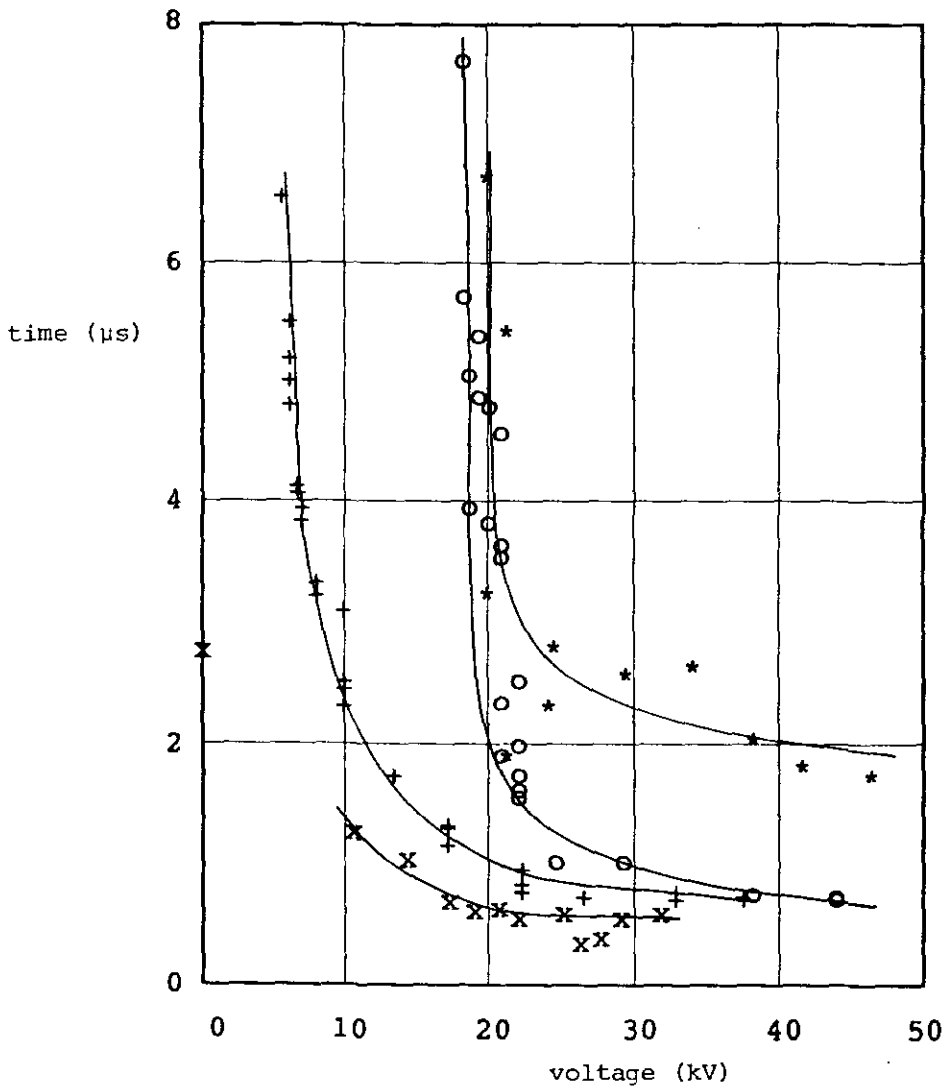

Figure 10. Time delay for the first optical peak. Abscissa represents dc bias for 2.5 kV (--0--), 15.6 kV (--+--), 26 kV (--x--) pulses and crest coltage for pulse only (--*--) curves.

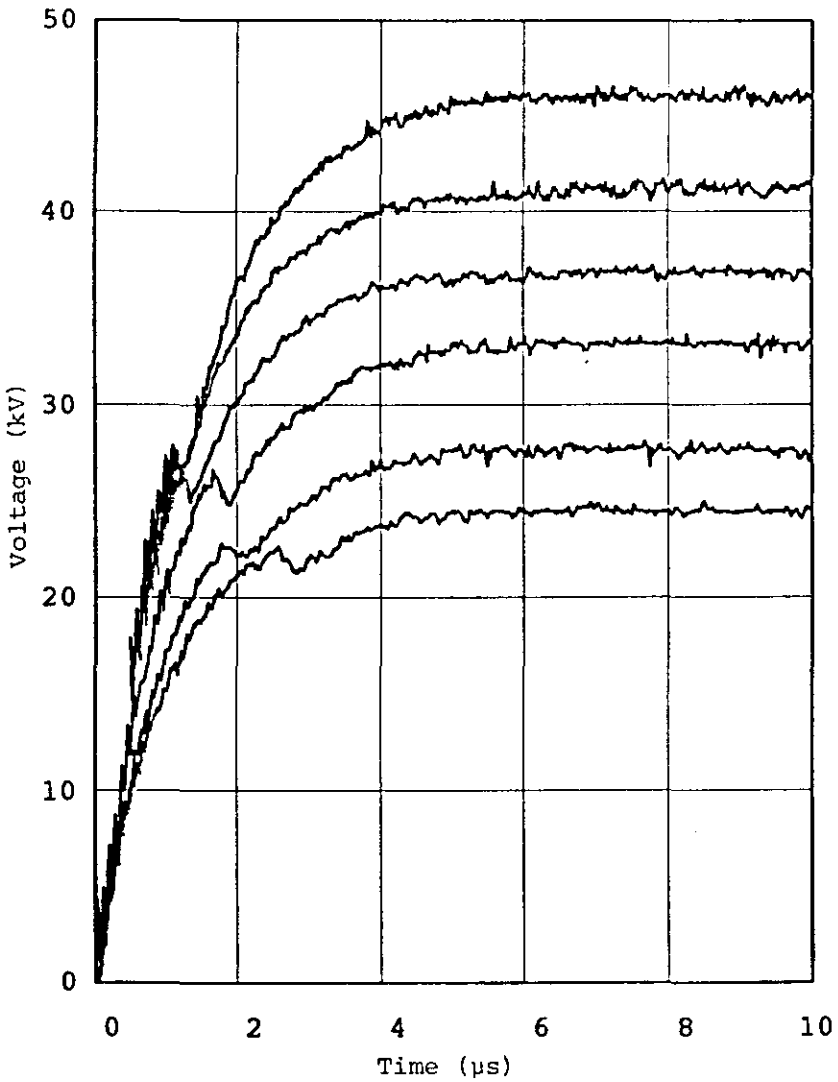

Figure 11. Voltage pulses showing the dip corresponding to emission of the light peak.

shows longer time delay at higher crest voltage. However, if the time taken by the pulse to reach the inception voltage is subtracted, this curve comes close to the lower one. Figure 12 can be used to divide the initial development of pulsed positive corona into two regions.

The first is the avalanche region (Mc Allister 1979) which is roughly between 20 and 26 kV total voltage. In this region the optical signal appears as several peaks with more or less randomly distributed intervals and amplitude. The time delay between the start of the electrical pulse and the first optical pulse can be several times the rise time of the electrical pulse. The statistical spread in the time delay is of the same order of magnitude as the delay itself (see figure 8a and 9a). In the avalanche region the current in the pulse is of the order of milli-amperes which is estimated from the dc current of the power supply. The second region, above 26 kV total voltage, shows a more consistent shape of the optical signal and a shorter time delay. As mentioned earlier now the current of approximately 1 ampere flows through the system. Here the corona is initiated through the development of streamers (Dawson 1965, Marode 1975, Gallimberti 1988).

One would have expected pulsed corona to behave differently when started from virgin gas and from dc glow. But our observations show that it is the total voltage applied to the corona wire which determines the inception time, no matter how we reach this voltage. Therefore, pulsed positive corona in cylindrical configuration can be initiated without appreciable delay for 26 kV and higher voltages. In the inception region, however, as we go down in voltage the inception time increases asymptotically.

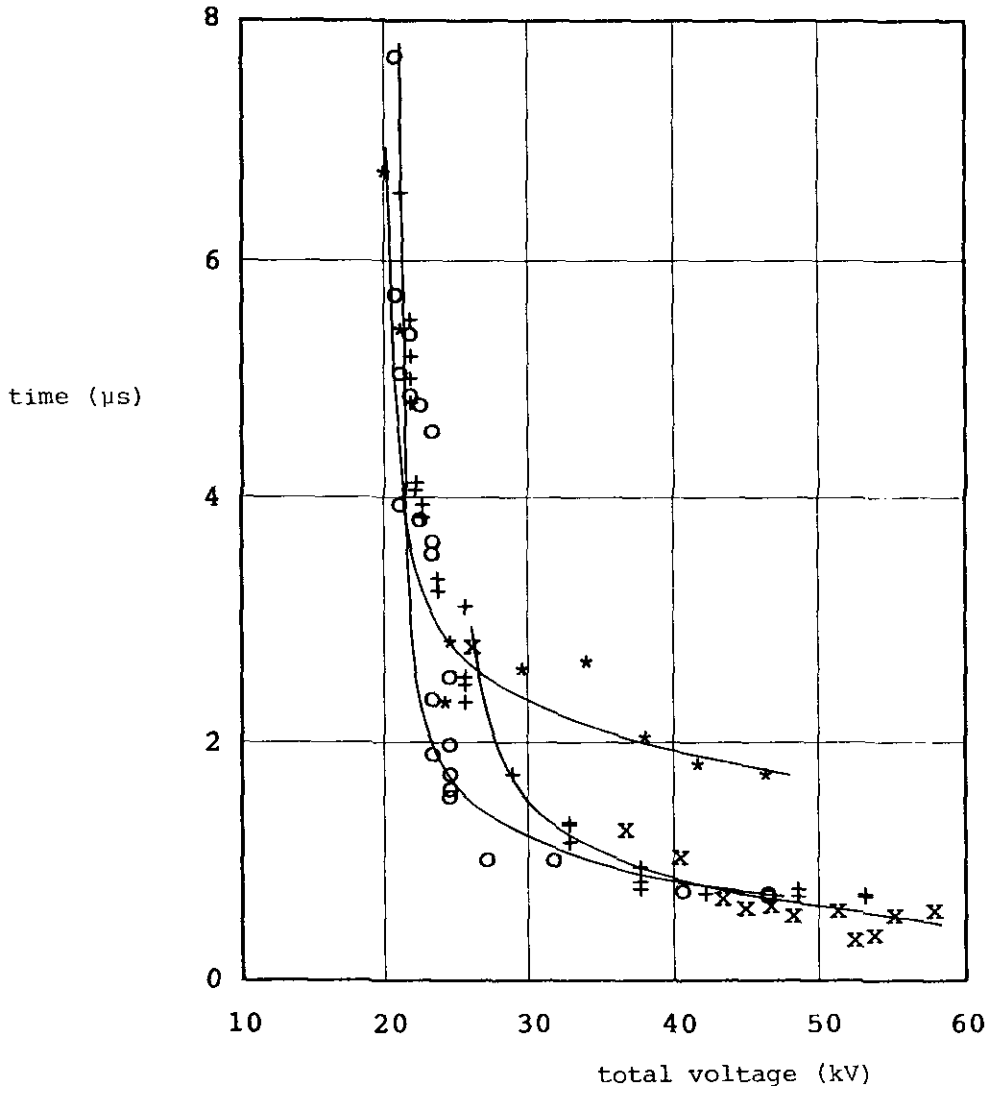

Figure 12. Time delay for the first optical peak as a function of the total applied voltage. 0-7.5 kV pulse, (-+-) 15.6 kV 15.6 kV pulse, (-x-), 26 kV pulse, (-*) only pulse.

4. Conclusions

We have studied positive corona in air to delineate the initial behaviour of corona discharges generated by fast electrical pulses. The corona is generated by superimposing fast rising (4 μs rise time) electrical pulses on dc bias. Several combinations of pulse and dc bias are used. The peak pulse voltage is raised from 2.5 kV to 46 kV whereas the dc bias is controlled independently. The light emitted from the corona is used to evaluate the time for corona initiation. We arrive at the following conclusions from our experimental investigations:

1. The light emitted from the dc corona follows the current voltage characteristic.
2. When the corona is initiated by superimposing either 2.5 kV or 15.6 kV pulses on the dc bias, in the inception region several light peaks are emitted from a burst of fast, electrical discharges called avalanches. The pulses have a time delay and jitter that is longer than the rise time of the electrical pulse. With the increase of the total voltage the time delay and jitter are reduced. The optical intensity and the discharge current increase considerably due to streamer formation.
3. Above 26 kV pulses highly reproducible optical signals are emitted by the streamers even if there is no dc bias.
4. In the streamer regime two light peaks of different amplitude are detected seperated in time by an intervening dark period. The amplitude of the first light peak is always considerably higher then that of the second.
5. The time delay for corona initiation depends on the total voltage applied to the stressed wire electrode whatever may be the ratio of pulse to dc voltage.
6. The envelopes made for the optical signal emitted from 300 different corona shots under various combinations of the pulse and dc bias show that not only the time delay but also the jitter in optical signal is reduced by raising the total voltage.
7. In the avalanche regime the time delay for corona initiation decreases sharply with the applied voltage while in the streamer regime beyond a total voltage of 26 kV the corona can be initiated almost instantaneously.
8. Current of ≈1 ampere is estimated from the dip in voltage pulse corresponding to the emission of optical signal from streamers.

Part II. Negative corona

1. Introduction

In electrostatic precipitators handling high resistivity fly ash a combination of pulse and dc voltage provides an effective method of controlling the problem of back corona (Nelson and Salasoo, 1987, Lagarias et al. 1981). A pulser generating fast rising high voltage pulses can be used for retrofitting (Masuda and Hosokawa 1988, Gallaer 1983) the conventional dc energized precipitator plants. The features of the negative corona formed under the combined stress of the pulse and dc voltage are different from those of the dc corona alone. The current is distributed more evenly over the length of the wire (Kloth 1987). The corona initiation and the field dependant migration of the charge carriers are influenced not only by the voltage but also by the rise time of the electrical pulse. Salasoo et al (1985) have developed a two-dimensional numerical model for such a case to obtain electric field and movement of the charged particles. Their experimental measurements support the model calculations for the integrated current under both steady and pulsed voltages, but not for the Trichel pulse frequencies. Thanh (1979) has observed larger number of Trichel pulses during the rising part of the voltage pulse than in the decaying part. This is attributed to the electric field resulting from the combined effect of the applied field and the net space charge. For the pulsed voltage these are time dependent parameters at a given point in space.

Anode directed streamers can be launched at high electric fields. The transport equations dealing with the formation and propagation of the streamers have been solved numerically by Dhali and Williams (1987). The two dimensional flux-corrected transport algorithm used by them could handle strongly space-charge dominated conditions at the head of the streamers. Their investigations show that the electron density and its gradient at the head of the streamer increase with the applied field, which they find opposite to the case of the positive streamers.

The electrons heated by the high fields at the head of the streamers can dissociate the gas molecules during collisions to form active radicals. In flue gases NOx and SO2 react with the radicals produced by the energetic electrons and the acidic mists can then be removed. The streamer dominated pulsed coronas have been used by Masuda and Nakao (1986) to control NOx and by Clements et al (1986) for the combined

removal of NOx, SO2 and fly ash.

The corona initiation and its development in time is governed by the temporal variation of the electrical field. The pulsed corona can therefore envolve quite differently from the dc corona. For the pulse and dc voltage combined to generate the corona their relative magnitudes and also the pulse rise time play an important role. In the negative corona the electrons drift away from the high voltage cathode in the decreasing electrical field. Moreover, the negative ions formed by the attachment of electrons take substantial amount of time to move away from the active region near the cathode. The positive ions moving towards the cathode enhance the Laplacian field. Poli (1982) has used the concept of active volume to compare the statistical time lags for initiation of the negative and the positive pulsed coronas.

The aim of the present paper is to study the initial behaviour of the negative corona under various electrical conditions. The corona has been generated by imposing fast rising voltage pulses on the dc bias. In the inception region the light signal due to the development of avalanches is observed but at higher voltages stronger signals from streamers are recorded.

2. Experimental set-up

The system used for the negative corona experiments is the same as described in part I of this paper. But the polarities of the high voltage power supplies have been reversed to apply negative voltage at the corona wire. Figure 1 shows the electrical circuit which is used to generate the negative electrical pulses superimposed on the negative dc bias. The pulse rise time and its half width are usually independent of the crest value over a wide range. The pulse rise time can be varied by changing the 10 kΩ resistor in series with the spark gap. For the present experiments we have used either 10 kΩ or 0 Ω resistor. When the resistor is 10 kΩ the pulses have a rise time of 3.5 μs which decreases to 0.6 μs by shorting the resistor. In both the cases the pulse repetition rate is kept constant at 5 pulses per second.

An optical fibre and photomultiplier combination is used to measure the light signal emitted from the corona. The integrated light signals from a cylindrical volume around the corona wire is detected since the lens

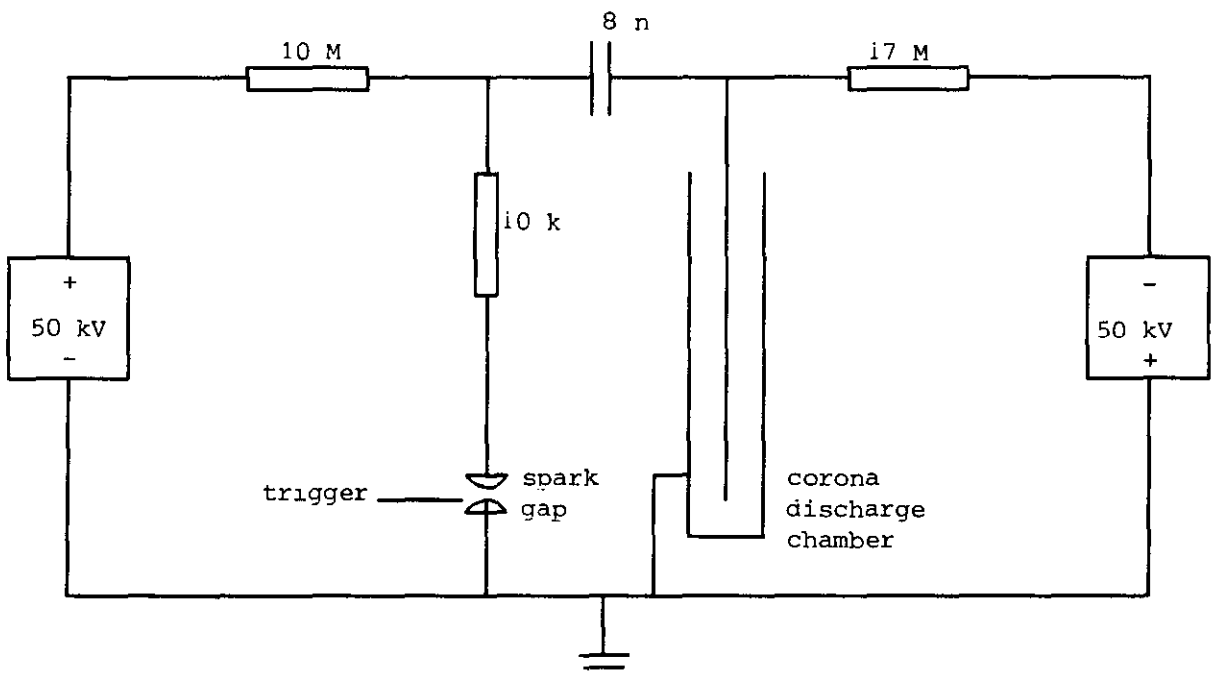

Figure 1. Electrical circuit to generate negative pulsed corona. Facility made available by the High Voltage Laboratory of the University.

fixed in front of the fibre focusses light on the fibre from this volume. In this manner we have studied the initial behaviour of the corona development. The photomultiplier output signal is recorded on the Hewlett-Packard 16500A logic analyser mainframe operated in oscilloscope mode using the 16531A plug-in module. The sampling time of this digital scope is 2.5 ns. The signal is stored on floppy discs to process the data by a computer. However, the signal for -26.4 kV pulses superimposed on dc bias is recorded on Tektronix oscilloscope 7603 having 25 ns sampling time. The other experimental details are given in part I of this paper where the positive corona is discussed.

3. Results and Discussion

The experimental conditions are given in Table II.1 together with the electrical pulse and dc combinations for which the experiments have been performed. For the pulsed corona the start of the electrical pulse has been taken as a reference for measuring the time. The electrical pulse voltage refers to its crest value. The time delay of the optical signal therefore includes 0.5 μs, mostly due to the delay in the long fiber cable.

3.1. dc corona characteristics

The corona system is characterized by plotting current as a function of dc voltage applied to the corona wire. The current voltage characteristic shown in figure 2 have been obtained by increasing the negative voltage continuously upto 45 kV and then decreasing it towards zero. The current and voltage signals are recorded on the two channels of the Nicolett oscilloscope 4024 C. Then x-y plot is made from this data on a computer. The current-voltage characteristics for the increasing and decreasing routes of the negative voltage are marked by the arrows pointing in the upward and downward directions respectively. The current has higher values while the voltage is brought down towards zero from -45 kV. It may be due to the combined effect of surface modification of the wire by sputtering, some changes in the gas composition and the residual charges left around the wire by the corona formed because of the rising negative voltage (corresponding to the lower part of the curve).

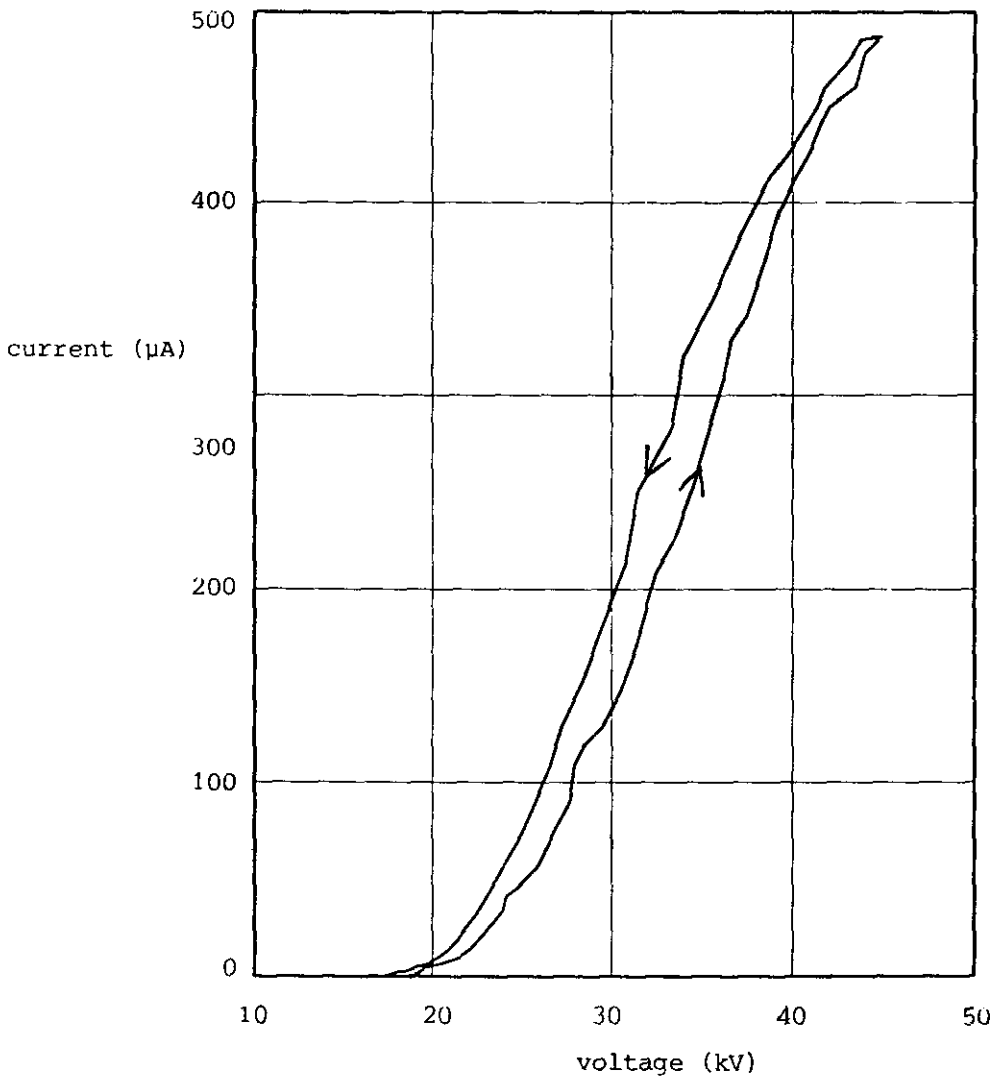

Figure 2. dc current-voltage characteristic of negative corona.
The arrows indicate the direction of the voltage variation.

It is evident from the figure that the corona inception voltage changes from - 18.5 kV to - 17.2 kV during the descending part of the characteristics. Since motion of the charge carriers is now opposite to that of the positive corona, there is no transition region of the type observed in part I for the positive corona near the inception. The mechanism for the development of the negative corona is essentially different as compared to the positive corona (Ramakrishna et al. 1989).

3.2. Optical signal emitted from pulsed corona

The optical signals recorded from the negative pulsed corona for the electrical conditions mentioned in Table II.1 are shown in figures 3 to 7. We have recorded optical signals from many different voltage settings by raising the dc bias and/or pulse peak voltages. At least three light signals have been recorded for each combination of peak pulse and dc voltage applied to the wire in order to have an idea about the jitter in the signal. In this paper we have included only a few of the representative signals.

The traces presented in figures 3 - 7 have been displaced arbitrarily in the vertical direction to accomodate more than one trace in a figure. Nevertheless the magnitude of the optical peaks can be evaluated by referring to the scale marked in the respective figures. The ignition of the spark gap is always taken as t = 0 for the time scale. It must be remembered that the time delay in the optical fiber is approximately 500 ns.

The signals for figures 3 - 5 have been obtained by keeping the crest voltage of the pulse constant at -3.6 kV, -15 kV and -26.4 kV respectively but by raising the dc bias. The pulse peak voltage has been raised from -21.0 kV to -48.4 kV for figures 6(a) - 6(d). Two zones are evident from the signals of figures 3 and 4 for the electrical conditions corresponding to the corona inception region. In the first zone starting from a time 7.5 μs in the top trace of figure 4a the optical signal has a regular structure with a time period of 48 ns. This seems to be the signal from Trichel pulses. There is another light peak of comparable amplitude of 8.5 μs. When the dc bias is raised the periodic structure slowly dies out but the second peak

Table II.1. Experimental parameters for pulsed negative corona

Medium : Air
Temperature: 21 *C (average)
Pressure : Atmospheric

S.No.	Electrical Pulse			DC (kV)
	crest voltage	rise time	half width	
	kV	μs	μs	
1	-3.6	2.3	320	-18.4 to -38.6
2	-15.9	3.5	430	-6.1 to -38.2
3	-26.4	3.5	430	0 to -33.5
4	-23.9 to -48.4	3.5	430	0
5	-26.4	0.6	460	0 to -38.1

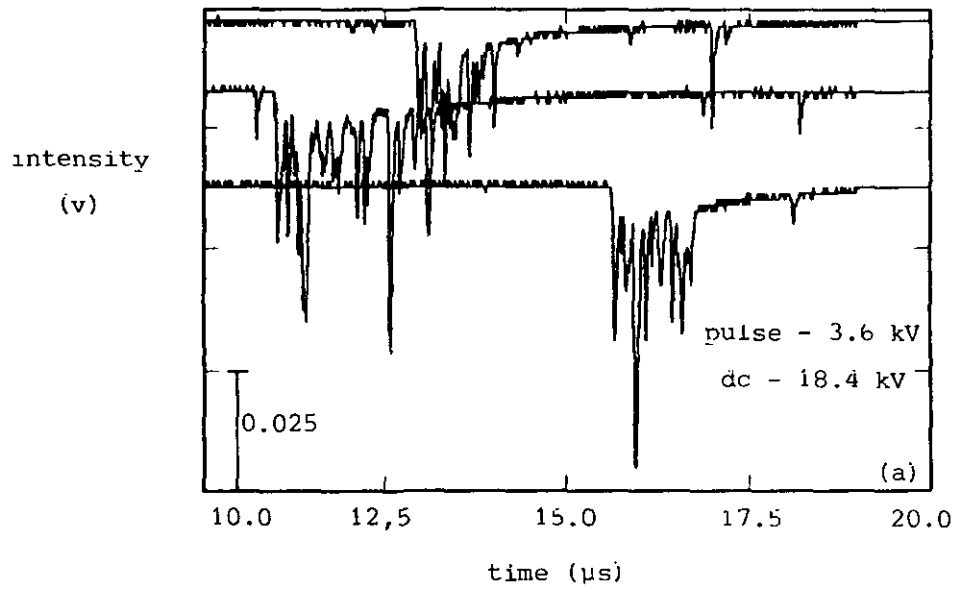

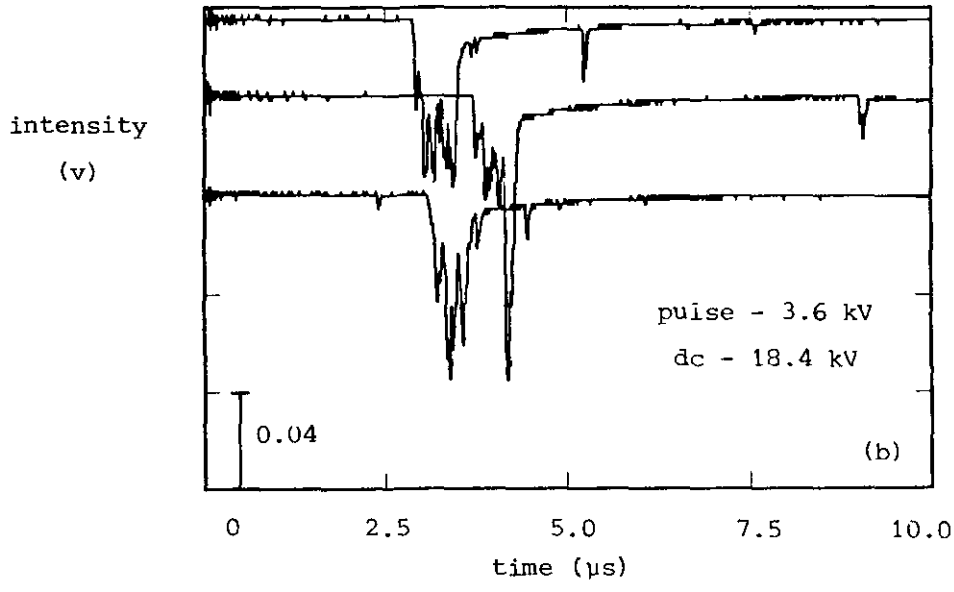

Figure 3. Optical signals emitted from negative pulsed corona generated with -3.6 kV electrical pulse superimposed on dc bias. The bias used is marked on the respective figures.

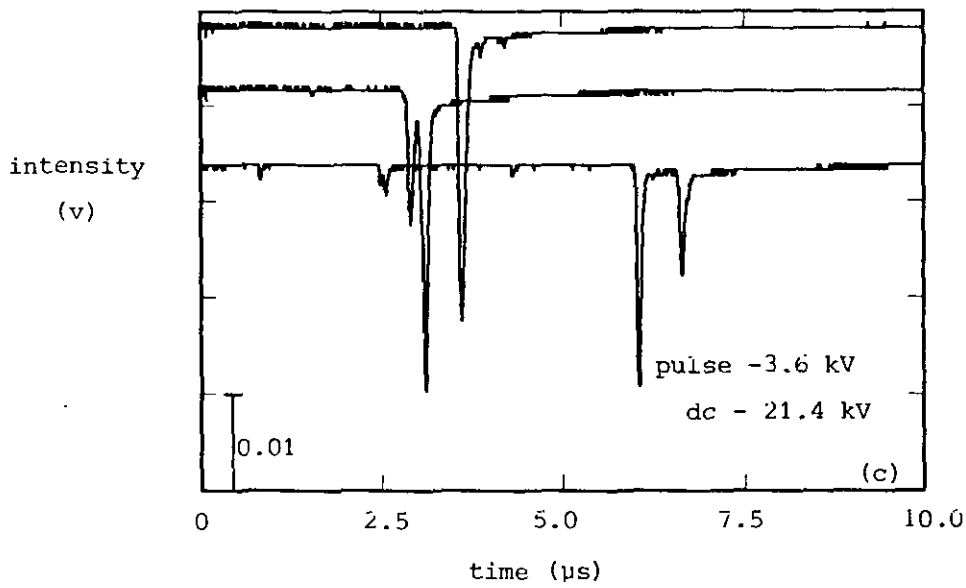

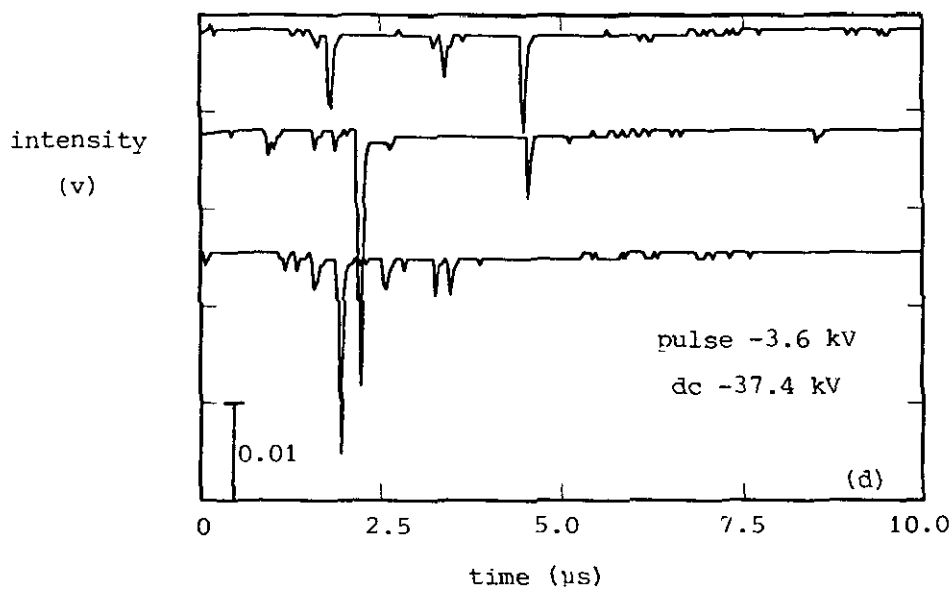

Figure 3. continued.

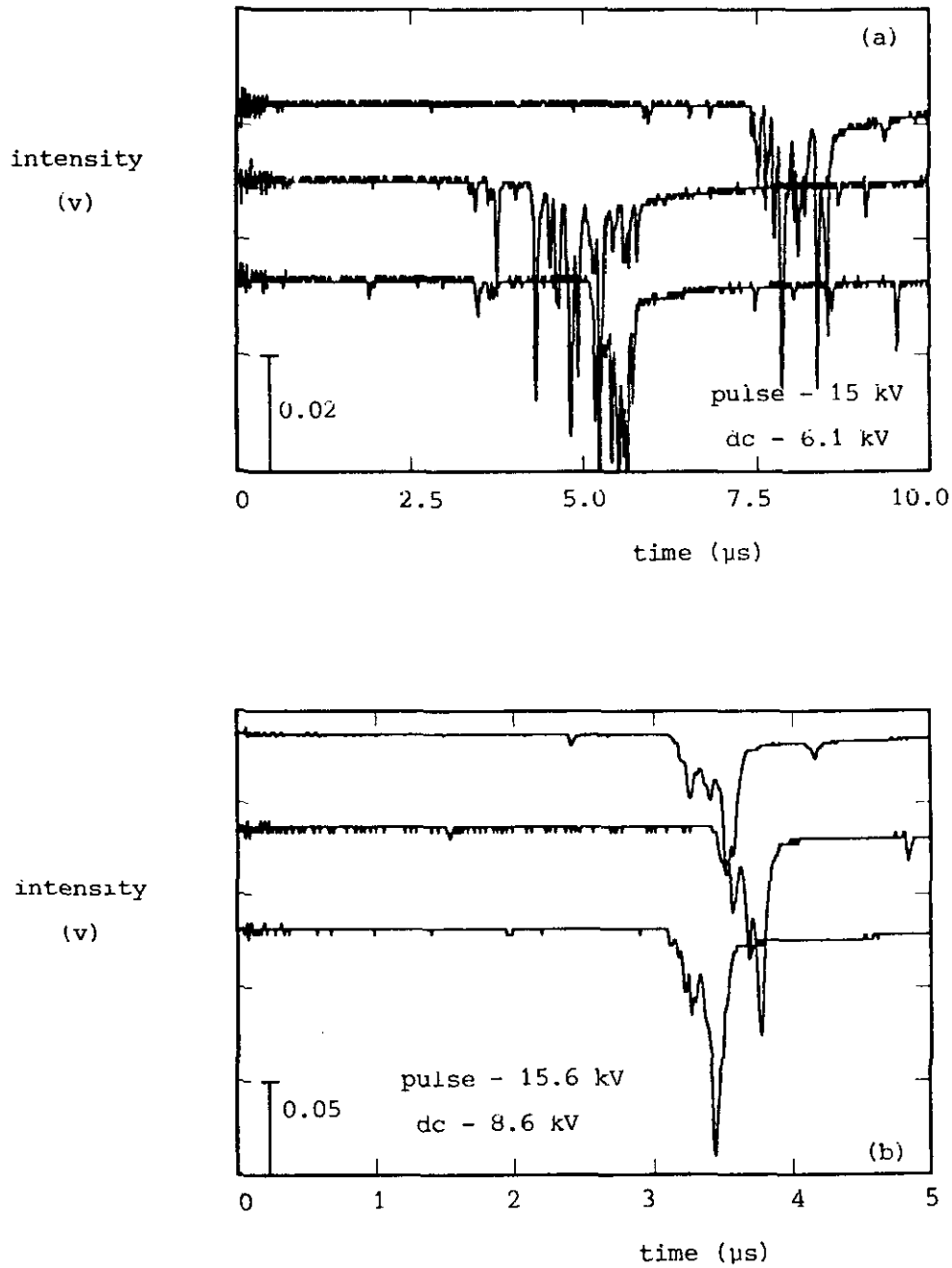

Figure 4. Optical signal emitted from negative pulsed corona generated with -15 kV electrical pulse superimposed on dc bias. The bias used is marked on the respective figures.

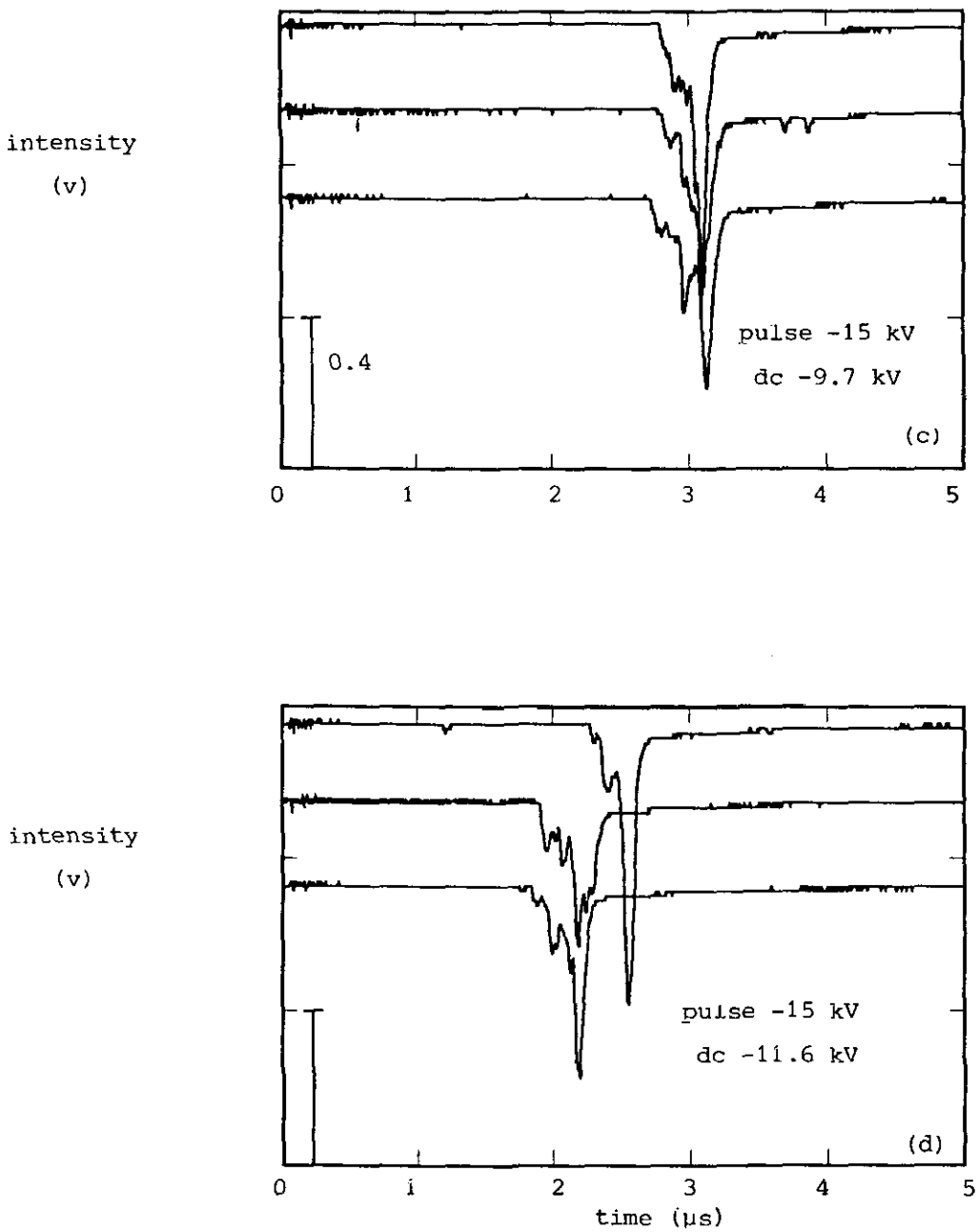

Figure 4. Continued.

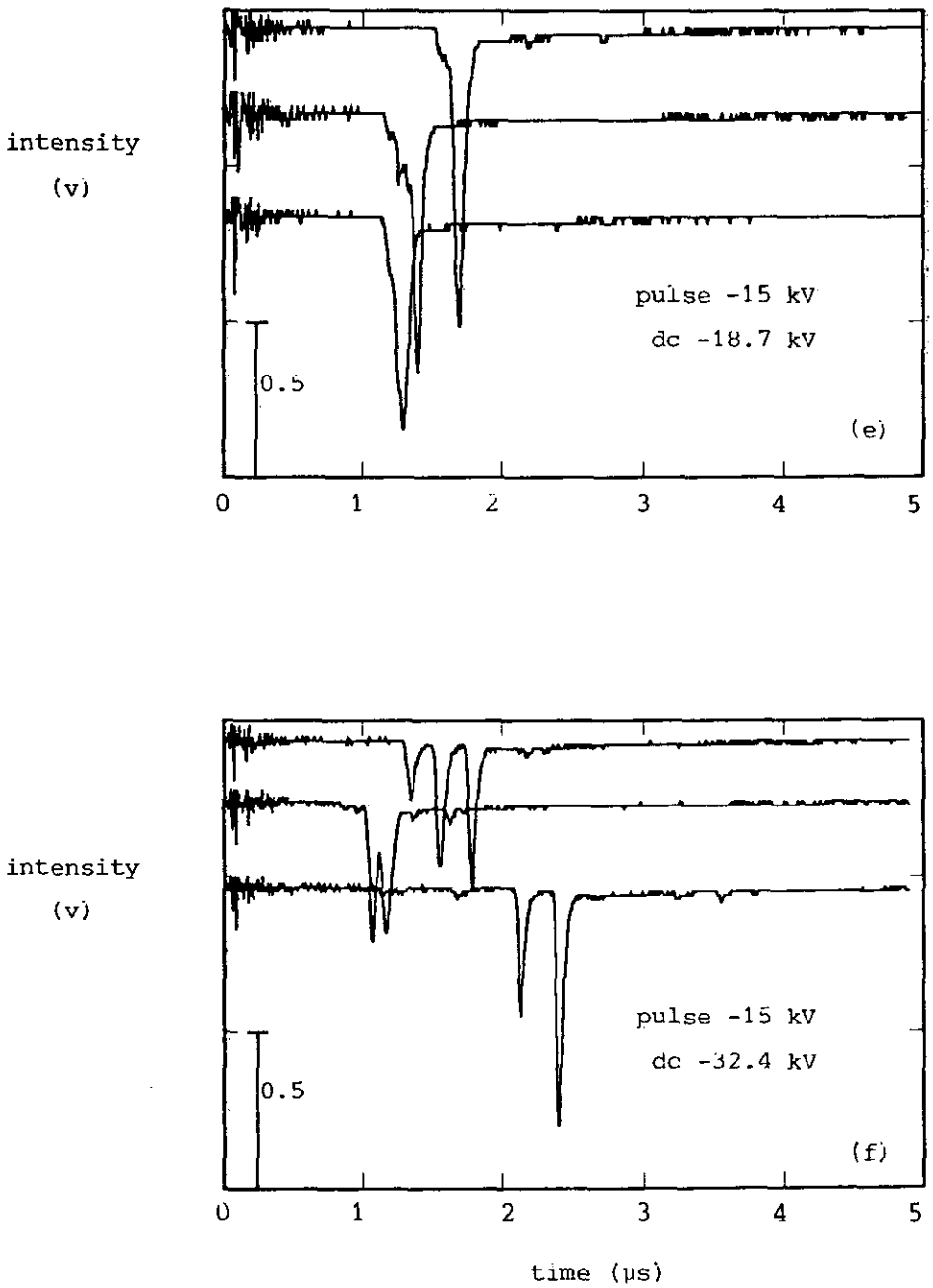

Figure 4. Continued.

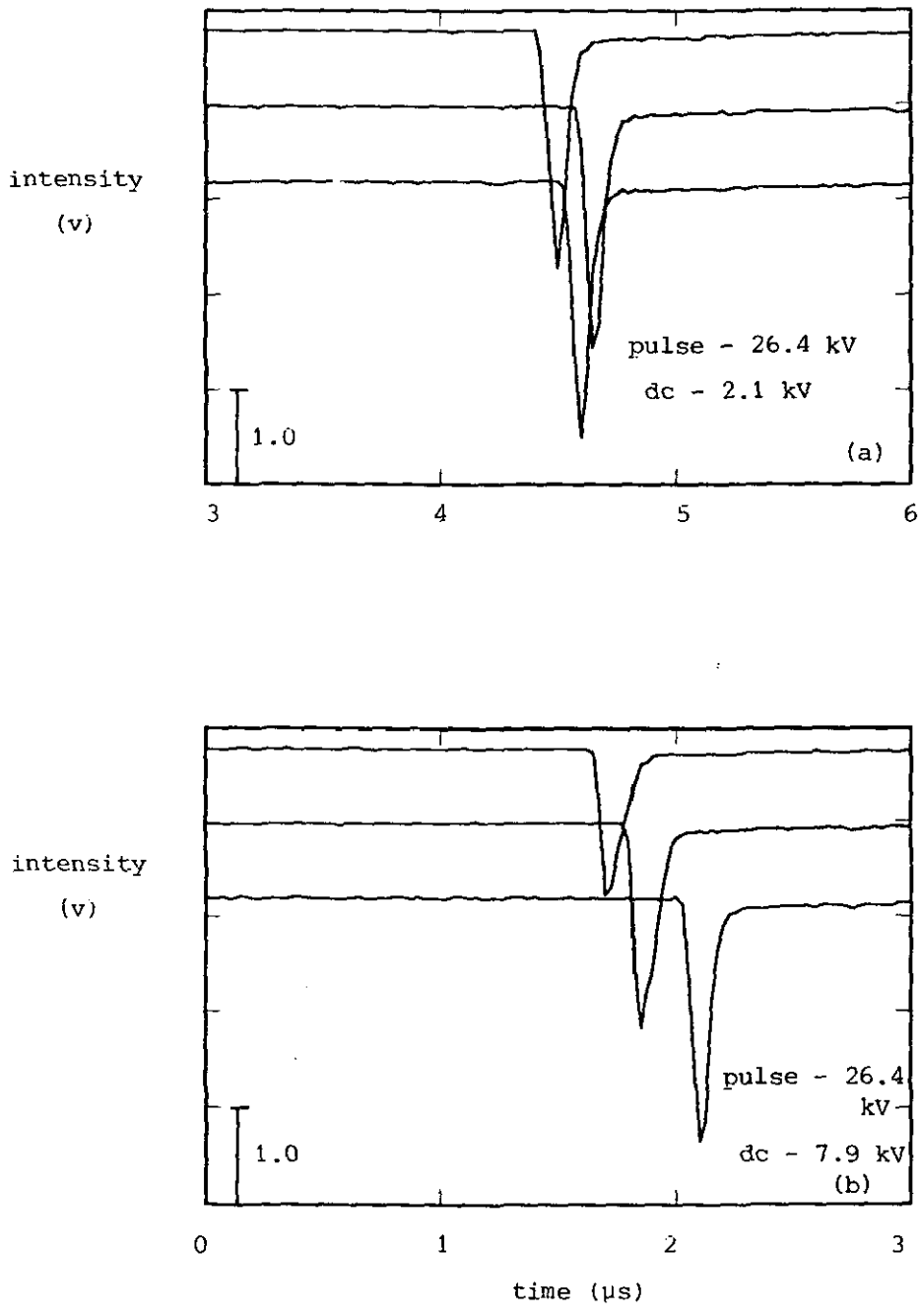

Figure 5. Optical signal emitted from negative pulsed corona generated with -26.4 kV electrical pulse superimposed on dc bias. The bias used is masked on the respective figures.

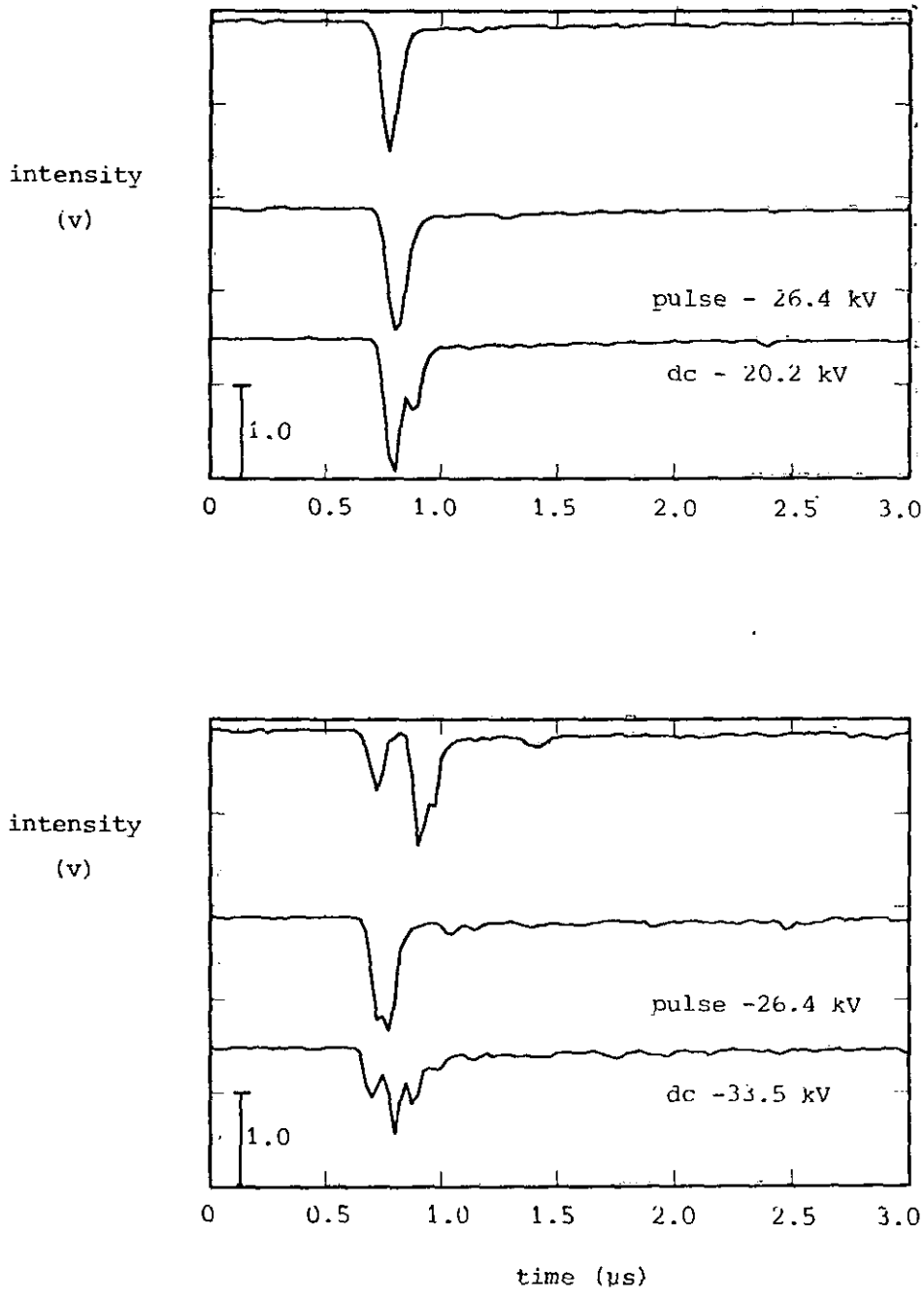

Figure 5. Continued.

grows. As the total potential on the wire goes up the time delay between the trigger of the electrical pulse and the appearance of the light signal reduces gradually.

It is interesting to note from figures 3 and 4 that the signal with periodic structure disappears when the dc bias exceeds the corona inception voltage (figures 3c, d and 4f). Now a few distinct stronger light peaks are observed which may be from the anode directed negative streamers (Dhali and Williams 1987). It means the negative corona behaviour is significantly influenced by the initial conditions, particularly by the charge density, in the vicinity of the stressed electrode.

When the pulse voltage is raised to -26.4 kV a single light peak is normally observed as is shown in figures 5(a) - 5(c). Under these conditions the crest value of the pulse voltage itself is substantially higher than the corona inception voltage. Hence it seems that the negative streamers are launched at the outset. But at a dc bias of -33.5 kV depicted in figure 5(d) the single well defined peak is no longer observed. The multiple light peaks seem to be from several succesive streamers seperated in time possibly from different places along the wire.

The optical signal emitted by the pulsed corona without any dc bias is shown in figure 6. The signal from the avalanches is observed in the inception region for -21 kV peak voltage (figure 6a). In absence of the dc bias we have noticed an interesting behaviour of the negative pulsed corona. Figures 6(b) and 6(c) are for the same -30.5 kV crest value of the electrical pulse. All other experimental conditions are also identical. Even though the corona is sometimes initiated after a lapse of 10 to 148 μs (figure 6b) and suddenly the light signal is detected merely after a few microsecond (figure 6c) from the start of the electrical pulse. The jitter in the optical signal also goes down when the corona is formed with a small time delay. A similar behaviour can be seen in figures 6(d) and 6(e) at higher pulse voltages. Eventually the time delay progressively decreases with the voltage.

The rise time of the electrical pulse is expected to play an important role in the corona initiation because of its impact on the electron

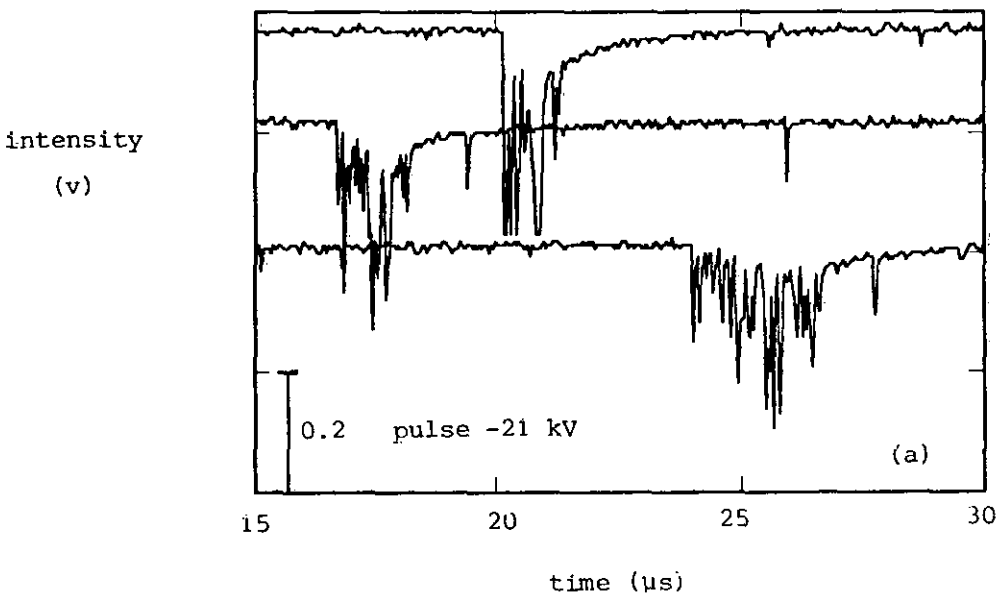

Figure 6. Optical signal emitted from negative pulsed corona generated with electrical pulse only. The crest value of the pulse used is marked on the respective figures.

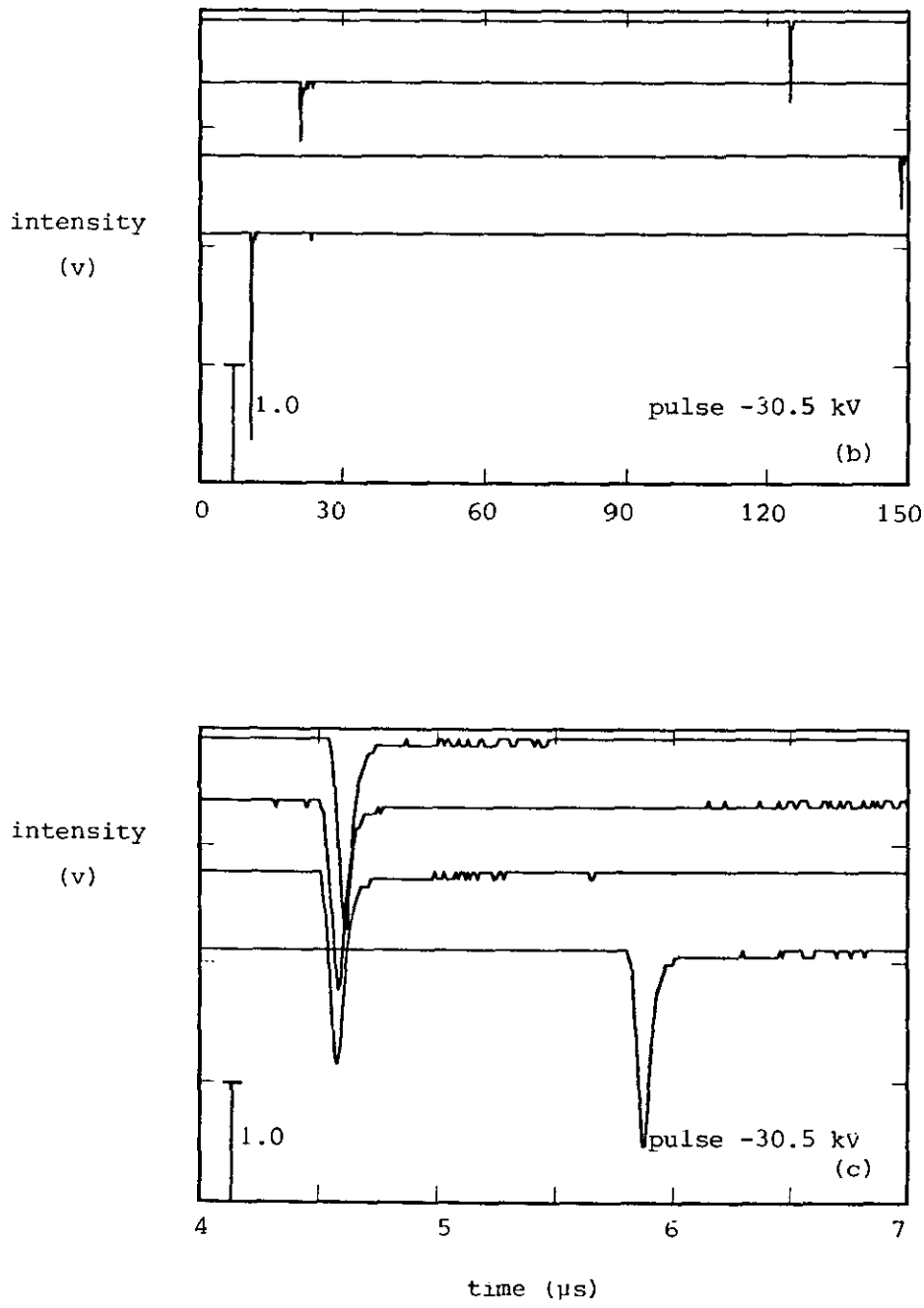

Figure 6. Continued.

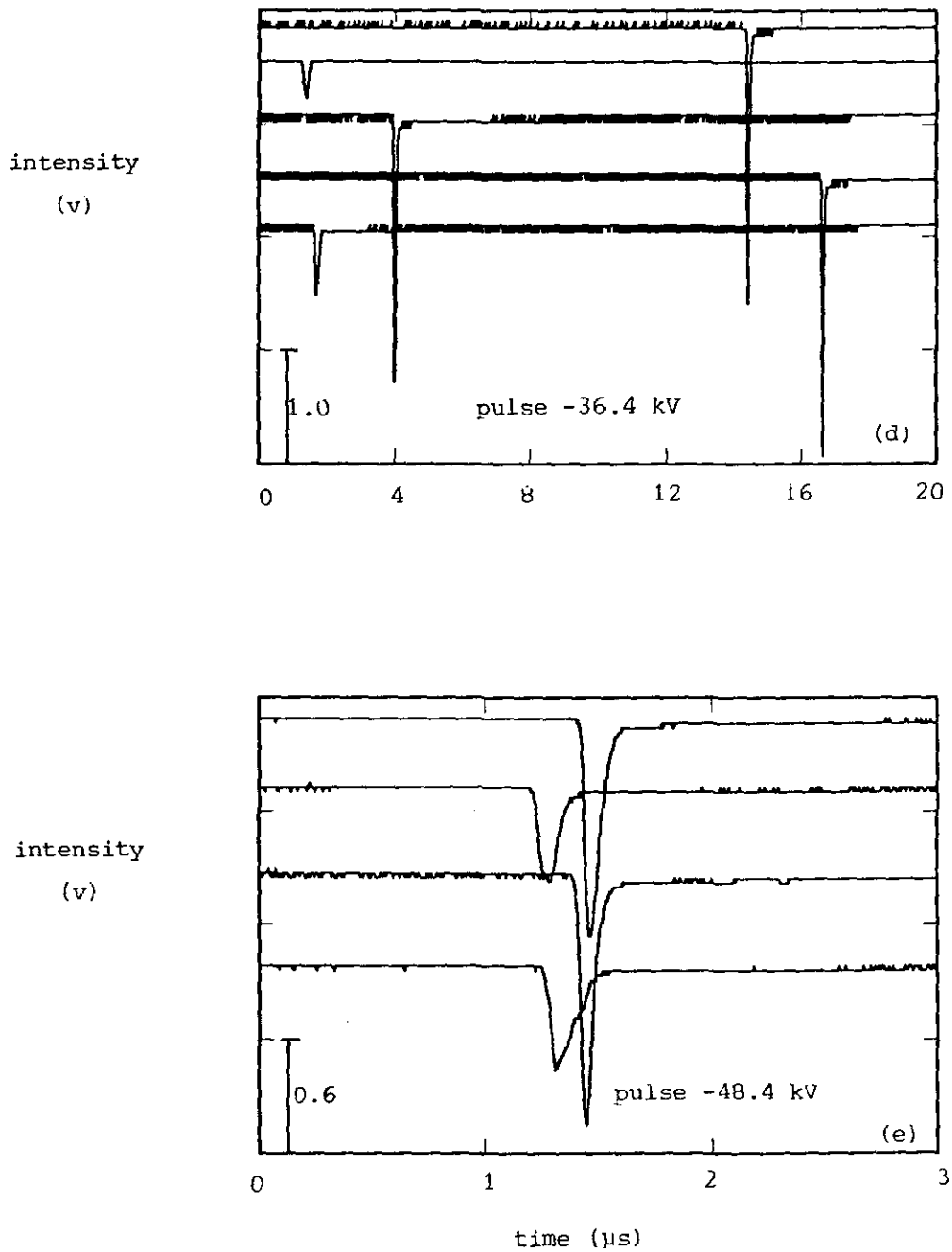

Figure 6. Continued.

temperature. We have therefore repeated our experiment for -26.4 kV electrical pulses; making the pulses to reach their crest value in 0.6 μs. These pulses are superimposed on negative dc bias to generate the corona. Figure 7 shows the light signal emitted from such a corona. As expected there is a considerable jitter in time for the optical signal at a low dc bias of -2.3 kV. The jitter as well as the time delay decrease when the negative bias is raised. The jitter is almost negligible for a dc bias of -35.3 kV. This is shown in figure 7(d). Since the dc bias is now considerably higher than the corona inception voltage, the charge carriers existing in the dc glow can trigger the streamers efficiently without any appreciable delay. A comparison between figures 7(d) and 5(d) shows that the faster rising electrical pulses give rise to more well defined streamers even if the pulses are superimposed on a high negative bias. No multiplicity of the light peaks is observed for -26.4 kV faster pulses.

In the streamer regime for positive corona we have observed two distinct light peaks of different amplitude and seperated by an intervening dark period (see part I). But in negative corona no secondary streamers are observed. Once the corona inception region is crossed by raising the negative potential, the light signal averaged along the line of sight of the optical fibre shows only a single peak corresponding to the negative streamers. However, the amplitude of the signal and its temporal position are functions of the applied potential.

3.3. Time for corona initiation

As mentioned earlier, we have taken triggering of the spark gap as reference for time measurements. This gives the time delay between the beginning of the voltage pulse and the appearance of the light signal form the corona. Since the nature and the amplitude of the optical signal has been varying under the different electrical conditions and our interest has been for the initial behaviour of the corona, we have measured the position (in time) for the first detectable major light peak.

The variation of the time delay is shown in figures 8 - 10 for different electrical conditions. The optical signals have been recorded

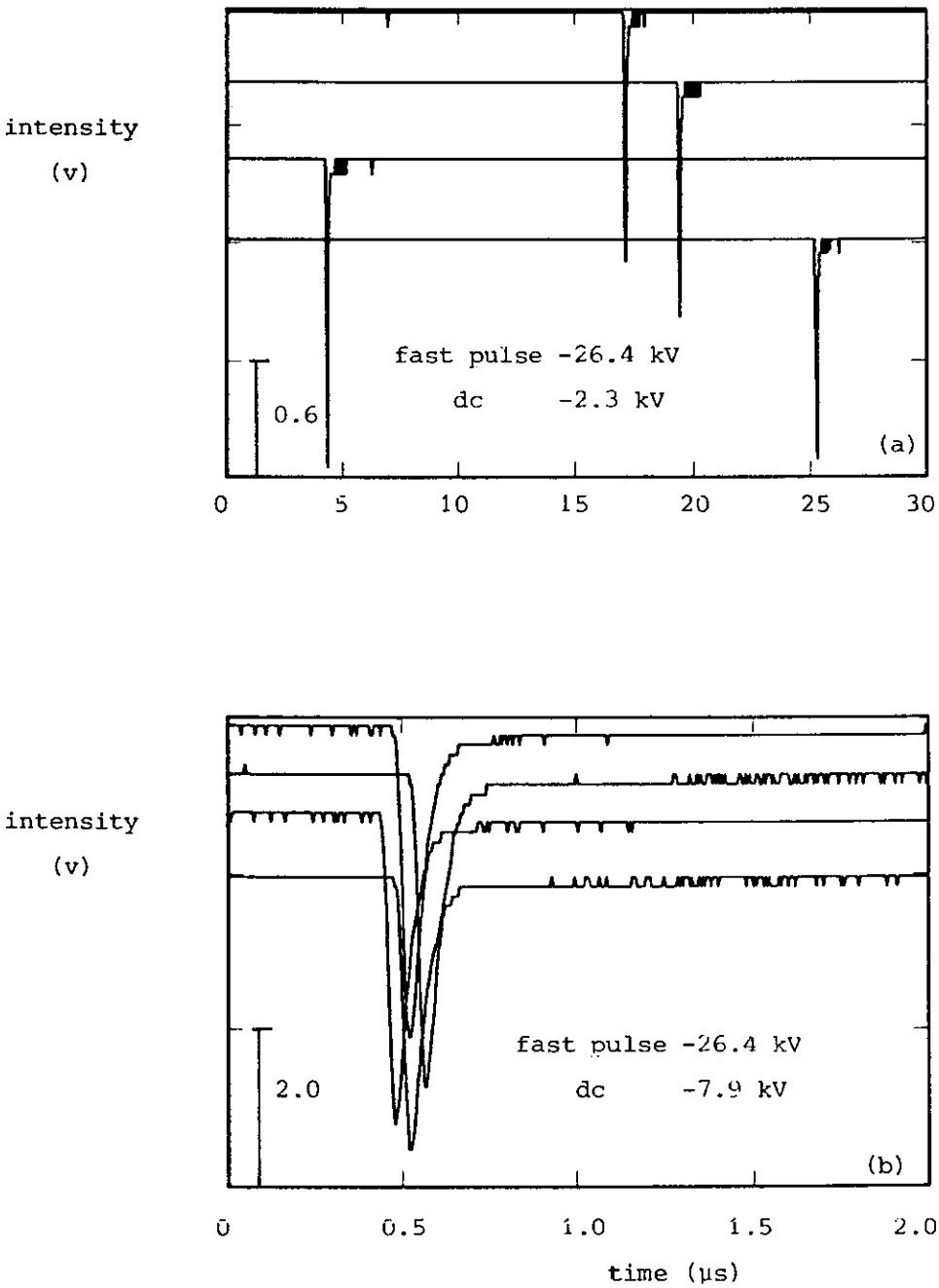

Figure 7. Optical signal emitted from negative pulsed corona generated with -26.4 kV faster electrical pulse superimposed on dc bias. The bias used is marked on the respective figures.

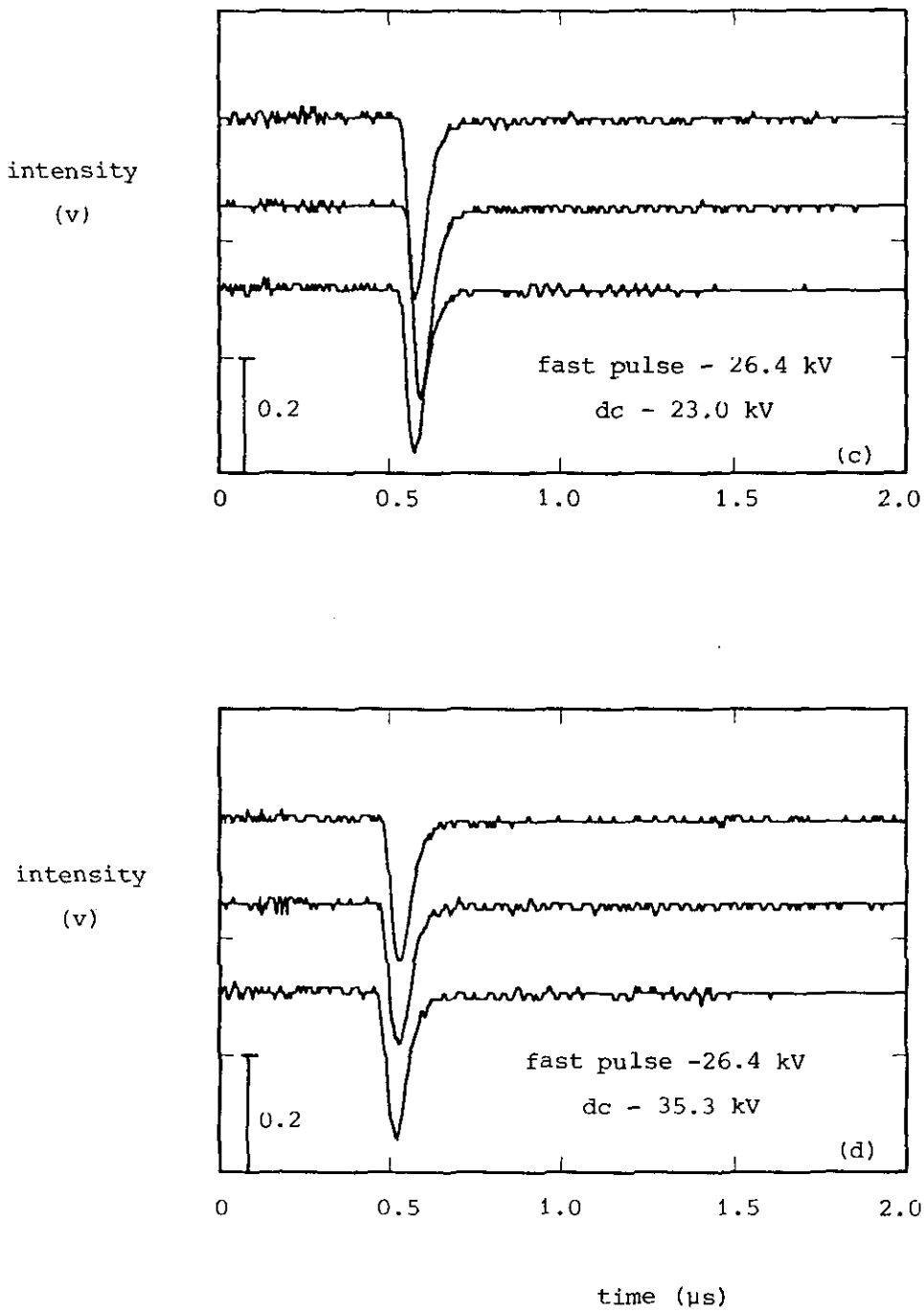

Figure 7. Continued.

for more than one trigger of the spark gap under identical experimental conditions. Therefore more than one point has been plotted at a given voltage. The spread of the points is referred to as jitter. The delay time from the optical fiber should be subtracted for calculating the actual time delay.

For figures 8(a) - 8(c) the crest value of the electrical pulse has been kept fixed at -3.6 kV, -15 kV and -26.4 kV respectively. The time delay is plotted as a function of the dc bias applied to the corona wire. All the three cases of figure 8 exhibit two regions. The first is the inception region where the time delay decreases sharply with the applied potential. And then follows the second region at higher voltages where the corona is initiated with negligible time delay. As we go from figure 8(a) to 8(c) the jitter in time reduces, particularly in the second region. It is evident from figure 8(c) that the jitter is very small between -10 and -25 kV dc bias. The increase in the jitter again after -25 kV is due to the appearance of more than one light peak.

Long and short time delays have been observed (figure 6) for the pulse only mode of corona generation. Figure 9 shows in a more complete form the variation of the time delay as a function of the crest value of the electrical pulse. The corona appears to be operating with three time scales merked I, II and III in figure 9. It suddenly switches from one time scale to another even if the experimental parameters are not altered. As the crest voltage is raised curves I and II come closer to each other. Very large time delays of upto 150 μs can be observed in the inception region. But when the dc bias is present on the wire the corona initiation does not take such a long time. The dc bias may be helping by clearing the space charge in the interpulse period.

A comparison is made in figure 10 between -15 kV, -26.4 kV and the pulse only mode of corona generation. Now the total voltage, i.e. the dc bias plus the crest value of the electrical pulse is taken as abscissa. The optical pulses having a maximum time delay upto 10 μs only have been included for the sake of clarity. It means the data points of curve I of figure 9 have been plotted in figure 10. Unlike the positive corona (see part I) the three curves do not merge into one another. The negative corona can be initiated at lower voltages by a

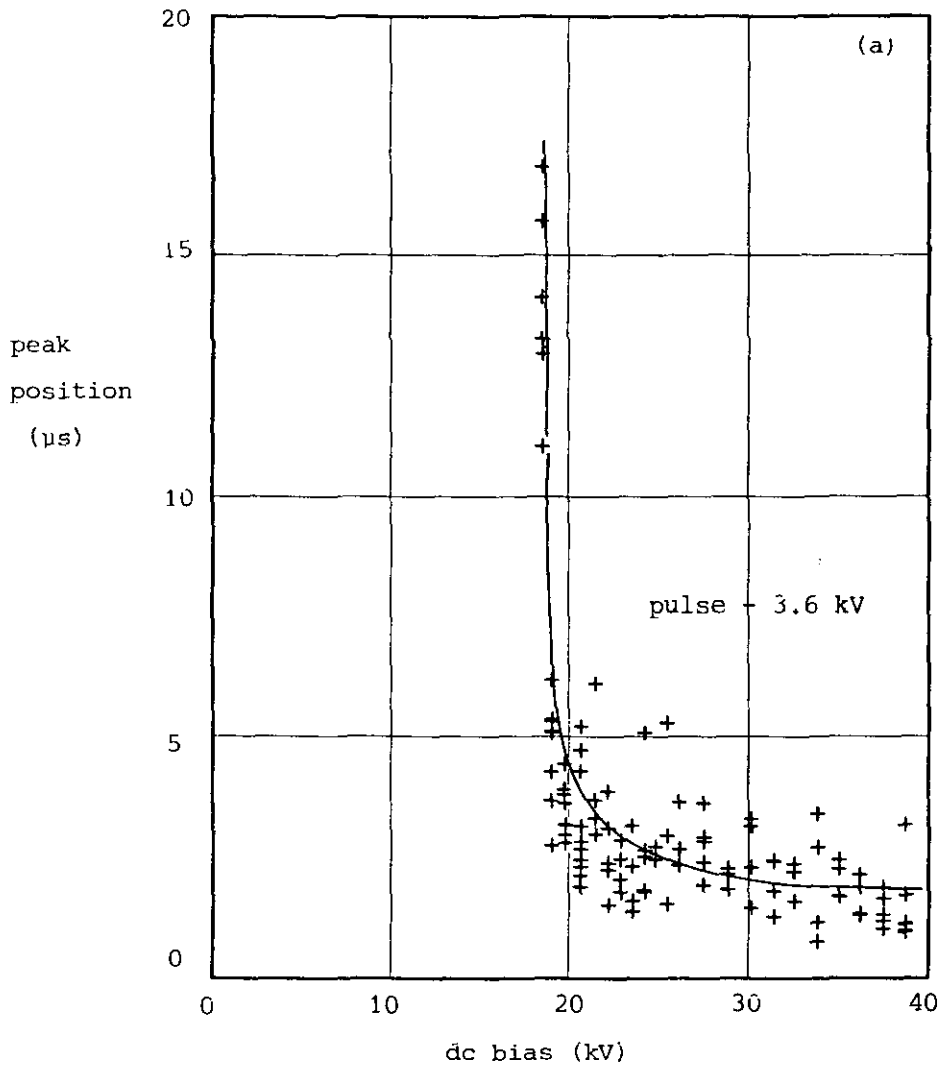

Figure 8. The time delay for optical peak as a function of dc bias. Triggering of the electrical pulse is the reference for the time delay measurements. Crest value of the electrical pulse voltage (a) -3.6 kV, (b) -15 kV and (c) -26.4 kV.

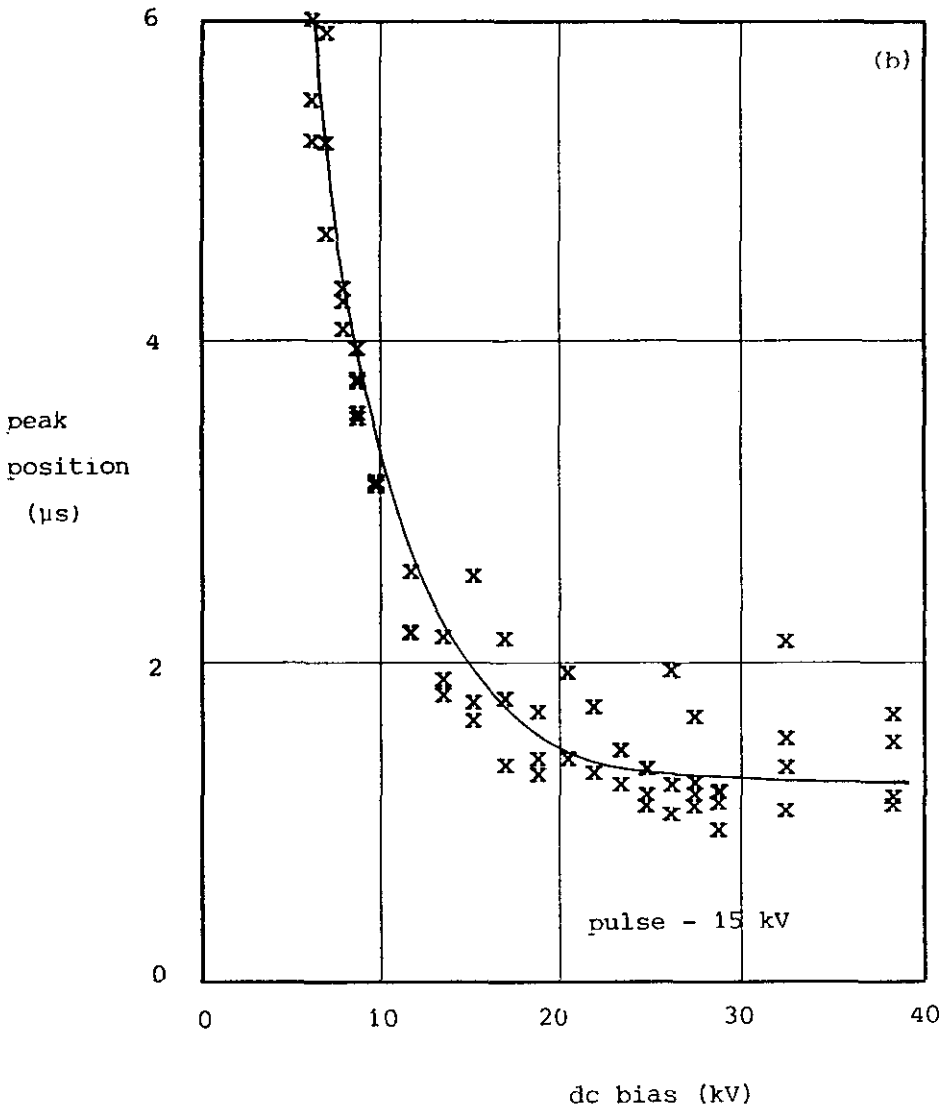

Figure 8. continued.

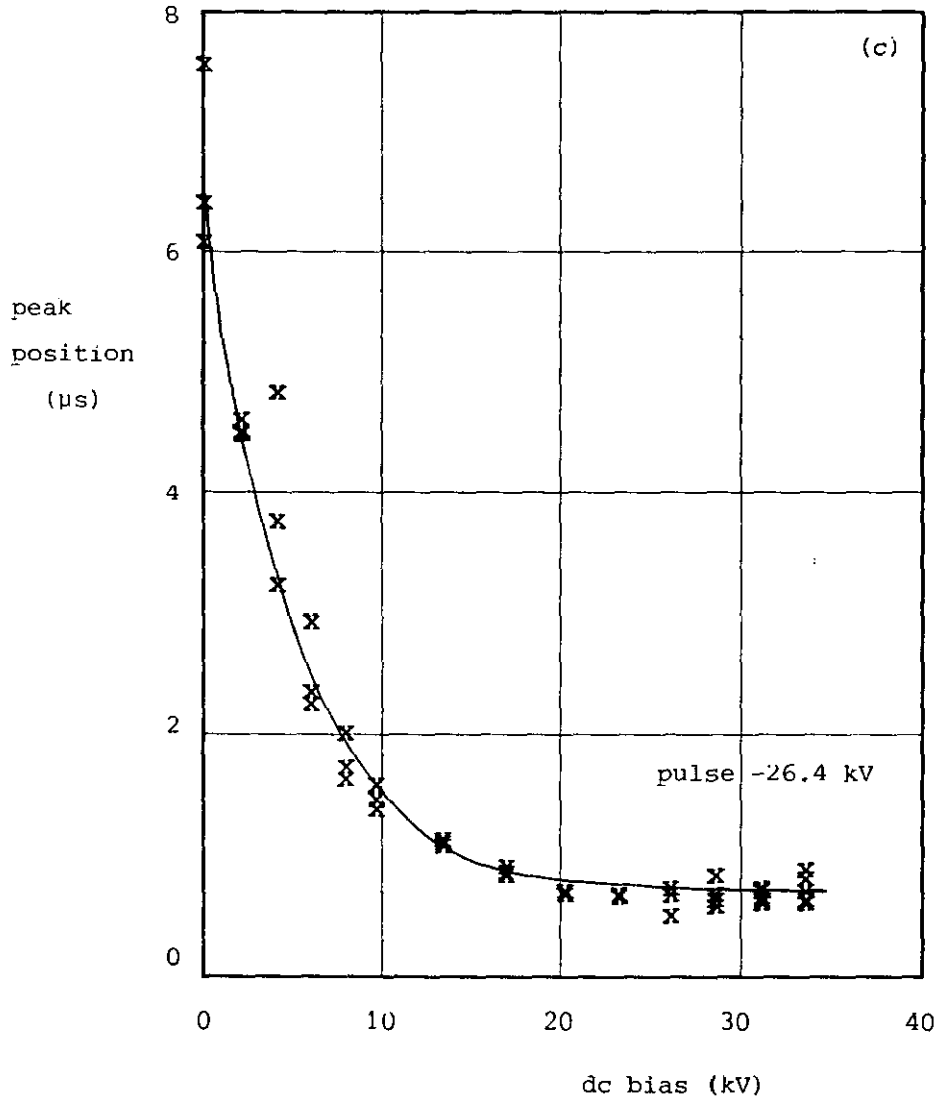

Figure 8. Continued.

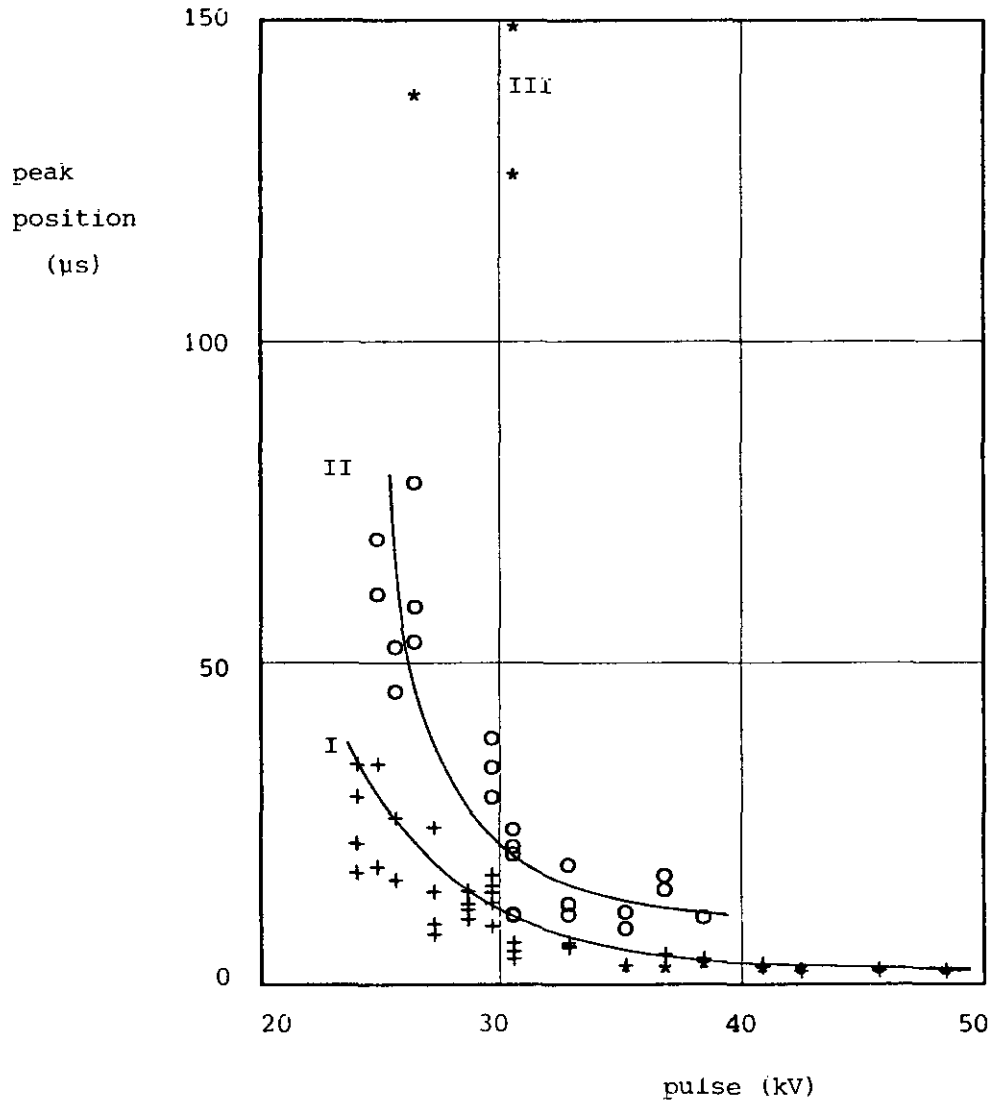

Figure 9. The time delay for optical peak as a function of crest voltage of electrical pulse. Triggering of the electrical pulse is the reference for the time delay measurements. Three modes of corona are marked by I, II and III.

combination of the dc bias and -15 kV electrical pulses. Once again we can see that the dc bias plays an important role for corona initiation. The difference between the three cases is not much at higher voltages.

3.4. Amplitude of optical signal

The light emitted from the corona gives an estimate of the corona activity. We have measured the amplitude of the first light peak only. It is shown in figure 11 as a function of the total voltage. The amplitude plotted for the case of electrical pulse only corresponds to the light signal represented by curve I of figure 9. Interestingly the amplitude of the light signal increases with the voltage upto a certain value and then it goes down at higher voltages. Such a decrease can partly be attributed to the appearance of more than one light peak from the multiple streamers. The maxima in the amplitude curves is observed to shift to lower total voltages as we go through the cases of -15 kV, pulse only and -26.4 kV.

The light signal for the three time modes of figure 9 also have different amplitudes. These amplitudes are shown in figure 12. The signal (marked with I) observed with the time delays comparable to the other cases studied in this paper shows a maximum in the amplitude at approximately -36 kV. But the amplitude of the signal corresponding to curve II (in figure 9) keeps on increasing with the crest value of the electrical pulse. We could not resolve significantly between curves I and II beyond - 38 kV. Therefore, the optical signal for -40 kV and higher voltages has been identified with curve I only. The points represented by * have been bracketed in III category on the basis of either very large (more than 125 μs) or very small ($\approx$0.5 μs) time delays together with the very small amplitude.

The behaviour of the optical signal emitted by superimposing -26.4 kV faster pulse (rise time 0.6 μs) on dc bias is different. In this case we have always observed a single well defined optical peak which should correspond to the coherent streamers. The amplitude of this peak is shown in figure 13. There is a sudden jump in the amplitude of the optical signal at 5.5 kV dc bias. After the jump there is a gentle decreasing trend in the amplitude right upto the highest dc bias we could reach with our experimental system.

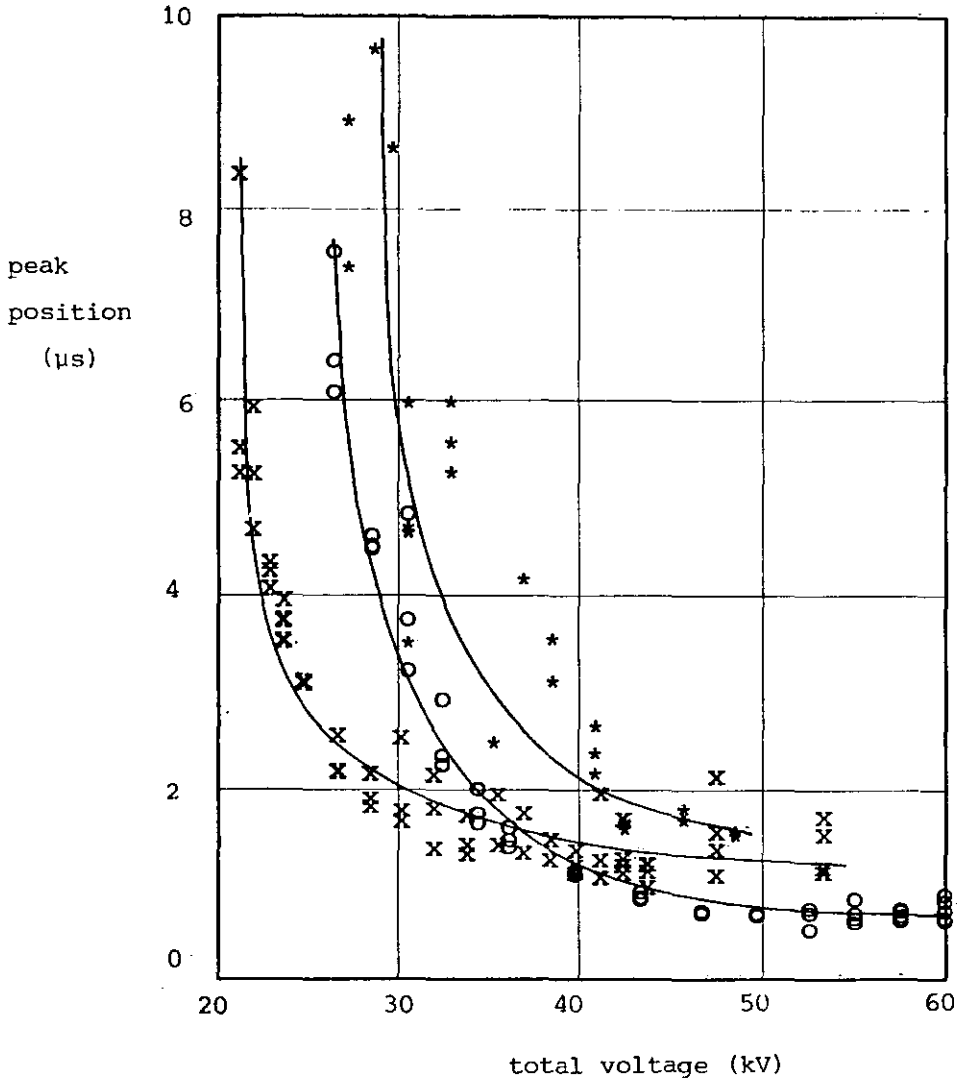

Figure 10. The time delay for optical peak as a function of the total applied voltage. -15 kV pulse (-x-), -26.4 kV pulse (-o-) and only pulse (-*-).

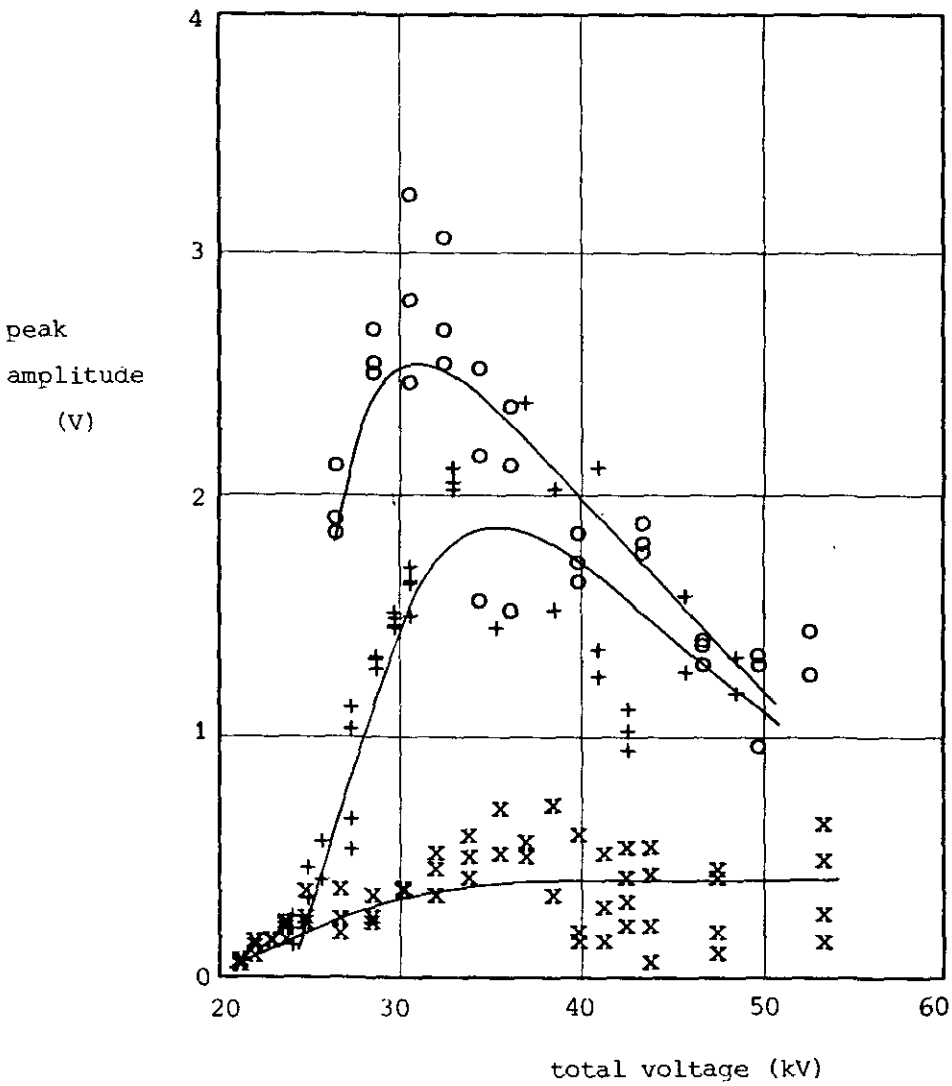

Figure 11. The amplitude of optical peak as a function of total applied voltage. -15 kV pulse (-x-), -26.4 kV pulse (-o-) and only pulse (-+-).

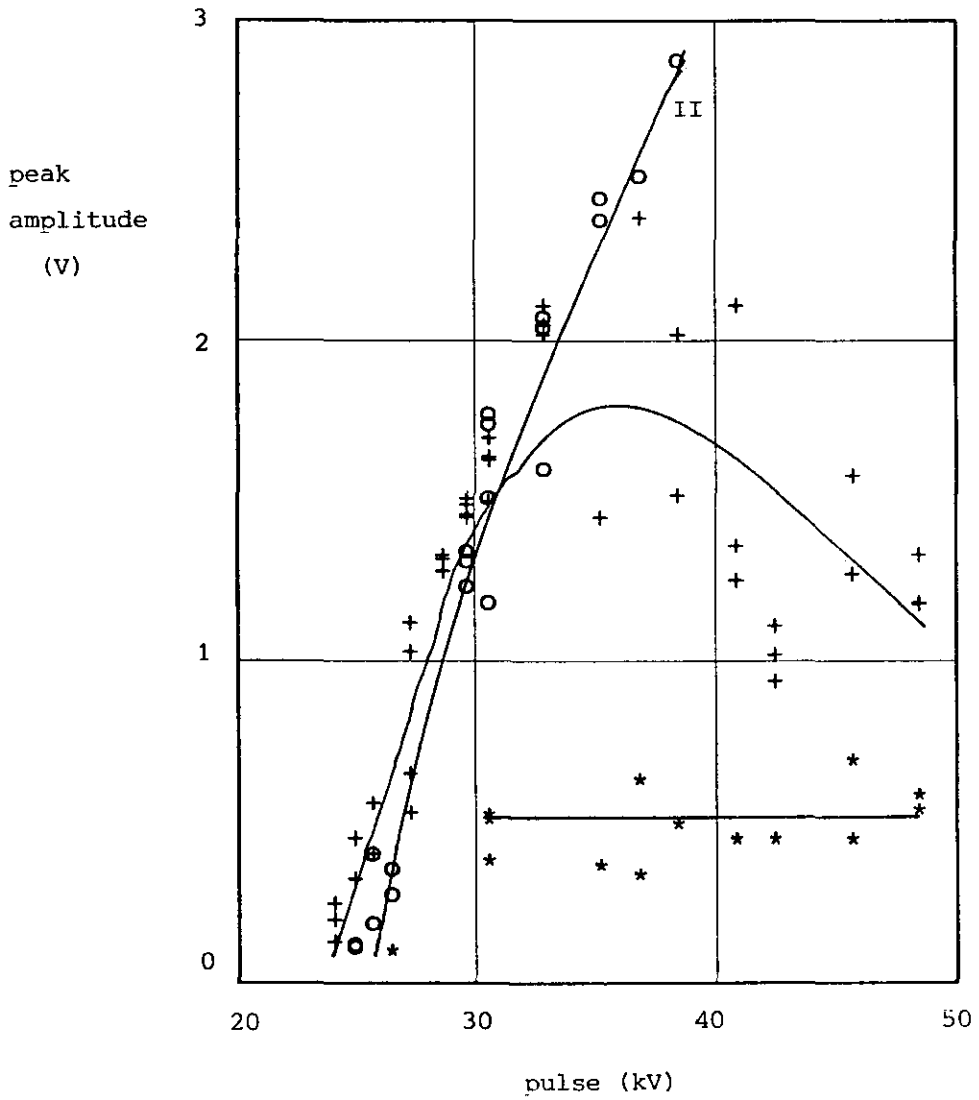

Figure 12. The amplitude of optical peak as a function of crest voltage. Three modes of corona are marked by I, II and III corresponding to figure 9.

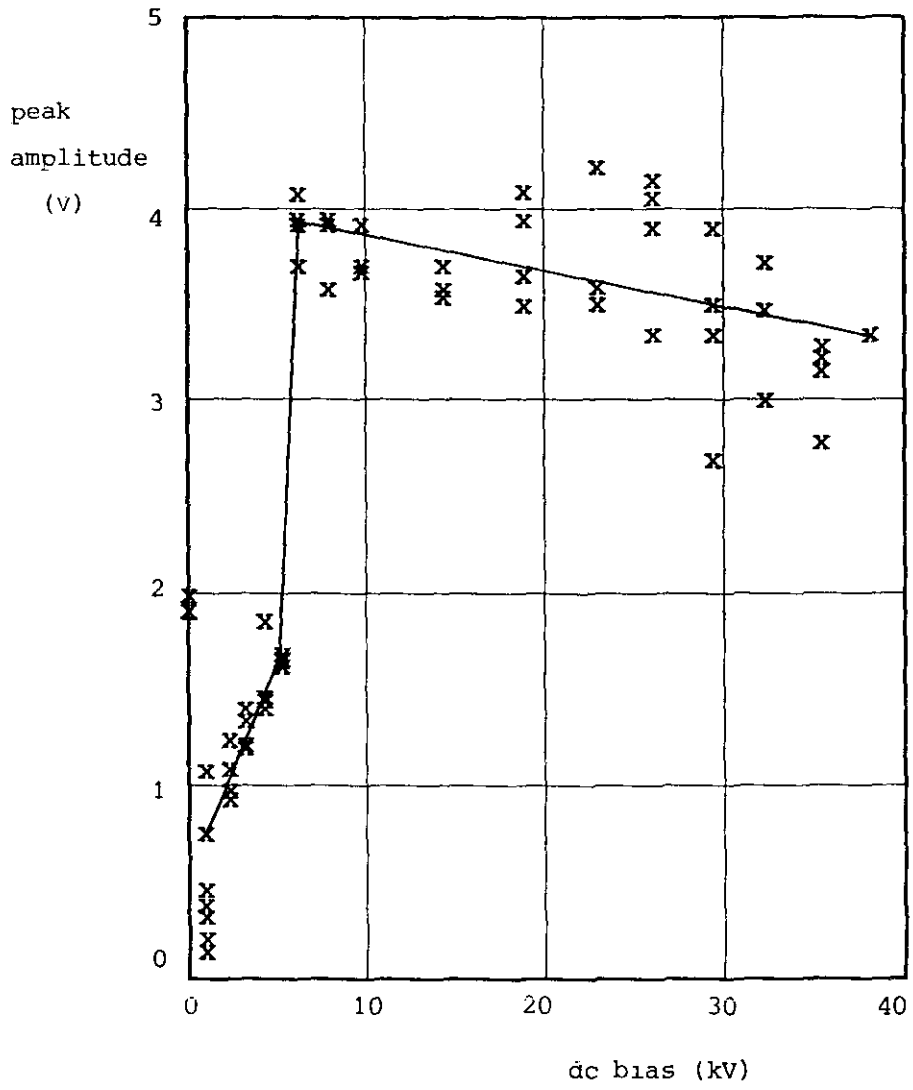

Figure 13. The amplitude of optical peak emitted from the negative corona generated by -26.4 kV faster electrical pulse. The rise time of the electrical pulse is 0.6 μs.

4. Conclusions

The recent industrial interest in pulsed coronas stems from the fact that these coronas can help to combat pollutants in flue gases. We have studied the initial behaviour of the pulsed negative corona in air by analysing the optical signal emitted from it. The temporal development of the corona around the stressed wire electrode is followed. The optical signal is detected by a photomultiplier looking axially along the wire. The crest value of the electrical pulse and the dc bias applied to the wire are varied independently. The voltage pulses have a rise time of either 3.5 μs or 0.6 μs. While varying the dc bias the crest voltage of the pulse is kept constant at either of -3.6 kV, -15 kV, -26.4 kV. But in the absence of the dc bias the pulse peak voltage is raised upto -48.4 kV. On the basis of the present experiments we may conclude as under:

1. The dc current voltage characteristic of the corona shows a hysteresis, the current being higher throughout for the decaying part of the voltage.
2. The light signal detected from the pulsed corona indicates that the corona is initiated by the build-up of avalanches evolving into anode directed streamers as the voltage is raised.
3. There is a significant influence of initial conditions on the behaviour of pulsed negative corona. The dc bias along with the electrical pulses helps to reduce the time delay for corona initiation which can otherwise be even 150 μs.
4. Multiple streamers are formed for a combination of pulse and dc voltage if the dc bias itself is more than the corona inception voltage.
5. Faster electrical pulses of - 26.4 kV with 0.6 μs rise time give well defined streamers for all values of the dc bias upto -38.1 kV.
6. In the inception region there is a sharp decrease in time delay with the total voltage applied to the wire. But in the streamer region the corona can be initiated almost instantaneously.
7. The time delay for negative corona initiation is determined not only by the total voltage, as observed for the positive corona, but also by the ratio of pulse and dc voltage.
8. The amplitude of the first significant light peak increases with the voltage to a maximum but goes down as the voltage is further

raised. For the faster pulses the amplitude jumps upwards by a factor of 2 at -5.5 kV dc bias and after that it has only gentle downward trend.

9. The transition from avalanche to streamer is at around 32 kV which follows from both the time delay and the amplitude. This value is higher than for the case of positive streamer (26 kV). Also the breakdown voltage for negative corona (> 65 kV) is higher than for the positive (56 kV).

The measurement of the time dependence of the optical emission is a good way to determine the behaviour of pulsed corona discharges under different conditions. It shows clearly the different regimes in which the discharge operates for different parameters such as the dc bias, the peak voltage and rise time of the electrical pulse. This can be of great help in working out the optimum parameters for practical applications. We are investigating pulsed corona discharges in flue gases for removal of pollutants from them. The optical measurements will be supplemented by fast current measurements. The Schlieren photography will be used to study the spatio-temporal development of the pulsed corona.

Acknowledgements

The facilities of the High Voltage Laboratory of the Eindhoven University of Technology were used to conduct these experiments. Appreciation is expressed to E.J.M. van Heesch for his expertise and to A.J.M.Pemen for his technical assistance.
The authors gratefully acknowledge valuable discussions with E.J.M. van Heesch, P.C.T. van der Laan, H.F.A. Verhaart and J.M. Wetzer. Secretarial assistance of M.H.A.J. van Rixtel-Kerkhoff is also acknowledged. This work has been performed with financial support from N.V. KEMA.

List of references

Allen, N.L. and M. Boutlendj
The threshold field for streamer propagation in air.
In: Proc. 9th Int. Conf. on Gas Discharges and their Applications, Venezia, 19-23 Sept. 1988.
Padova: Benetton Editore, 1988. P. 159-162.

Chalmers, D. and H. Duffy, D.J. Tedford
The mechanism of spark breakdown in nitrogen, oxygen and sulphur hexafluoride.
Proc. R. Soc. London Ser. A, Vol. 329, p. 171-191.

Civitano, L. and G. Dinelli, I. Gallimberti, M. Rea, R. Turri
Free radical production by corona discharges in a DeNOx-DeSOx reactor.
In: Proc. 9th Int. Conf. on Gas Discharges and their Applications, Venezia, 19-23 Sept. 1988.
Padova: Benetto Editore, 1988. P. 603-606.

Clements, J.S. and A. Mizuno, W.C. Finney, R.H. Davis
Combined removal of SO_2, NO_x, and fly ash from flue gas using pulsed streamer corona.
In: Conference record 21st IEEE Industry Applications Society Annual Meeting, Denver, Colo., 28 Sept. - 3 Oct. 1986.
New York: IEEE, 1986. P. 1183-1190 and also: IEEE Trans. Ind. Appl., Vol. IA-25(1989), p. 62-69 (revised).

Dawson, G.A. and W.P. Winn
A model for streamer propagation.
Z. Phys., Vol. 183(1965), p. 159-171.

Dhali, S.K. and A.K. Pal
Numerical simulation of streamers in SF_6.
J. Appl. Phys., Vol. 63(1988), p. 1355-1362.

Dhali, S.K. and P.F. Williams
Two-dimensional studies of streamers in gases.
J. Appl. Phys., Vol. 62(1987), p. 4696-4707.

Domens, P. and J. Dupuy, A. Gibert, R. Diaz, B. Hutzler, J.P. Riu
F. Rühling
Large air-gap discharge and Schlieren techniques.
J. Phys. D, Vol. 21(1988), p. 1613-1623.

Gallaer, Ch.A.
Electrostatic precipitator reference manual.
Palo Alto, Cal.: Electric Power Research Institute, 1983.
EPRI Report CS-2809

Gallimberti, I.
A computer model for streamer propagation.
J. Phys. D, Vol. 5(1972), p. 2179-2189.

Gallimberti, I.
The mechanism of the long spark formation.
In: Proc. 14th Int. Conf. on Phenomena in Ionized Gases, Grenoble, 9-13 July 1979, Vol. 2.
J. Phys. Colloq., Vol. 40, No. C7, Pt. 2(July 1979), p. 193-250.

Gallimberti, I.
Impulse corona simulation for flue gas treatment.
Pure & Appl. Chem., Vol. 60(1988), p. 663-674.

Heesch, E.J.M. van and J.N.A.M. van Rooy, R.G. Noij, P.C.T. van der Laan
A new current and voltage measuring system: Tests in a 150 kV and a 400 kV GIS.
In: Proc. 5th Int. Symp. on High Voltage Engineering, Braunschweig, 24-28 Aug. 1987. Chairman: Prof.Dr. H.C. Kärner, High Voltage Institute, Technical University Braunschweig. Paper 73.06.

Kline, L.E.
Calculations of discharge initiation in overvolted parallel-plane gaps.
J. Appl. Phys., Vol. 45(1974), p. 2046-2054.

Kloth, H.J.F. and E.J.M. van Heesch, P.C.T. van der Laan
Processes in pulsed electrostatic precipitators.
In: Proc. 5th Int. Symp. on High Voltage Engineering, Braunschweig, 24-28 Aug. 1987. Chairman: Prof.Dr. H.C. Kärner, High Voltage Institute, Technical University Braunschweig. Paper 91.05.

Lagarias, J.S. and J.R. McDonald, D.V. Giovanni
Assessment of the commercial potential for the high intensity ionizer in the electric utility industry.
J. Air Pollut. Control Assoc., Vol. 34(1981), p. 1221-1227.

Loeb, L.B. and J.M. Meek
The mechanism of spark discharge in air at atmospheric pressure.
J. Appl. Phys., Vol. 11(1940), p. 438-447 (part 1), 459-474 (part 2).

Marode, E.
The mechanism of spark breakdown in air at atmospheric pressure between a positive point and a plane.
J. Appl. Phys., Vol. 46(1975), p. 2005-2015 (part 1), 2016-2020 (part 2).

Masuda, S. and H. Nakao
Control of NO_x by positive and negative pulsed corona discharges.
In: Conference record 21st IEEE Industry Applications Society Annual Meeting, Denver, Colo., 28 Sept.-3 Oct. 1986.
New York: IEEE, 1986. P. 1173-1182.

Masuda, S. and S. Hosokawa
Pulse energization system of electrostatic precipitator for retrofitting application.
IEEE Trans. Ind. Appl., Vol. IA-24(1988), p. 708-716.

McAllister, I.W. and G.C. Crichton, E. Bregnsbo
Experimental study on the onset of positive corona in atmospheric air.
J. Appl. Phys., Vol. 50(1979), p. 6797-6805.

Mizuno, A. and J.S. Clements, R.H. Davis
A method for the removal of sulfur dioxide from exhaust gas utilizing pulsed streamer corona for electron energization.
IEEE Trans. Ind. Appl., Vol. IA-22(1986), p. 516-522.

Nelson, J.K. and L. Salasoo
The impact of pulse energization on electrostatic precipitation performance.
IEEE Trans. Electr. Insul., Vol. EI-22(1987), p. 657-675.

Phelps, C.T. and R.F. Griffiths
Dependence of positive corona streamer propagation on air pressure and water vapor content.
J. Appl. Phys., Vol. 47(1976), p. 2929-2934.

Poli, E.
A comparison between positive and negative impulse corona.
In: Proc. 7th Int. Conf. on Gas Discharges and their Applications, London, 31 Aug. - 3 Sept. 1982.
London: Peter Peregrinus, 1982.
PPL Conference, No. 20. P. 132-135.

Raether, H.
Die Entwicklung der Elektronenlawine in den Funkenkanal.
Z. Phys., Vol. 112(1939), p. 464-489.

Ramakrishna, K. and I.M. Cohen, P.S. Ayyaswami
Two-dimensional analysis of electrical breakdown in a nonuniform gap between a wire and a plane.
J. Appl. Phys., Vol. 65(1989), p. 41-50.

Salama, M.M.A. and H. Parekh, K.D. Srivastava
Corona inception under switching surge for point-to-plane long gaps.
J. Appl. Phys., Vol. 47(1976), p. 2915-2917.

Salasoo, L. and J.K. Nelson, R.J. Schwabe, R.W.L. Snaddon
Simulation and measurement of corona for electrostatic pulse powered precipitators.
J. Appl. Phys., Vol. 58(1985), p. 2949-2957.

Shelton, R.W. and J.A. Bicknell
A charge reconstruction technique for positive streamer growth measurement in quasi-uniform field.
In: Proc. 9th Int. Conf. on Gas Discharges and their Applications, Venezia, 19-23 Sept. 1988.
Padova: Benetton Editore, 1988. P. 177-180.

Spyrou, N. and C. Manassis
Spectroscopic study of a positive streamer in a point-to-plane discharge in air: Evaluation of the electric field distribution.
J. Phys. D, Vol. 22(1989), p. 120-128.

Suzuki, T.
Transition from the primary streamer to the arc in positive point-to-plane corona.
J. Appl. Phys., Vol. 42(1971), p. 3766-3777.

Thanh, L.C.
Characteristics of a corona system under negative direct and pulsed voltage.
J. Phys. D, Vol. 12(1979), p. 139-147.

Verhaart, H.F.A.
Private communication, 1989.

Eindhoven University of Technology Research Reports
Faculty of Electrical Engineering

ISSN 0167-9708
Coden: TEUEDE

(205) Butterweck, H.J. and J.H.F. Ritzerfeld, M.J. Werter
FINITE WORDLENGTH EFFECTS IN DIGITAL FILTERS; A review.
EUT Report 88-E-205. 1988. ISBN 90-6144-205-2

(206) Bollen, M.H.J. and G.A.P. Jacobs
EXTENSIVE TESTING OF AN ALGORITHM FOR TRAVELLING-WAVE-BASED DIRECTIONAL DETECTION AND PHASE-SELECTION BY USING TWONFIL AND EMTP.
EUT Report 88-E-206. 1988. ISBN 90-6144-206-0

(207) Schuurman, W. and M.P.H. Weenink
STABILITY OF A TAYLOR-RELAXED CYLINDRICAL PLASMA SEPARATED FROM THE WALL BY A VACUUM LAYER.
EUT Report 88-E-207. 1988. ISBN 90-6144-207-9

(208) Lucassen, F.H.R. and H.H. van de Ven
A NOTATION CONVENTION IN RIGID ROBOT MODELLING.
EUT Report 88-E-208. 1988. ISBN 90-6144-208-7

(209) Jóźwiak, L.
MINIMAL REALIZATION OF SEQUENTIAL MACHINES: The method of maximal adjacencies.
EUT Report 88-E-209. 1988. ISBN 90-6144-209-5

(210) Lucassen, F.H.R. and H.H. van de Ven
OPTIMAL BODY FIXED COORDINATE SYSTEMS IN NEWTON/EULER MODELLING.
EUT Report 88-E-210. 1988. ISBN 90-6144-210-9

(211) Boom, A.J.J. van den
H_∞-CONTROL: An exploratory study.
EUT Report 88-E-211. 1988. ISBN 90-6144-211-7

(212) Zhu Yu-Cai
ON THE ROBUST STABILITY OF MIMO LINEAR FEEDBACK SYSTEMS.
EUT Report 88-E-212. 1988. ISBN 90-6144-212-5

(213) Zhu Yu-Cai, M.H. Driessen, A.A.H. Damen and P. Eykhoff
A NEW SCHEME FOR IDENTIFICATION AND CONTROL.
EUT Report 88-E-213. 1988. ISBN 90-6144-213-3

(214) Bollen, M.H.J. and G.A.P. Jacobs
IMPLEMENTATION OF AN ALGORITHM FOR TRAVELLING-WAVE-BASED DIRECTIONAL DETECTION.
EUT Report 89-E-214. 1989. ISBN 90-6144-214-1

(215) Hoeijmakers, M.J. en J.M. Vleeshouwers
EEN MODEL VAN DE SYNCHRONE MACHINE MET GELIJKRICHTER, GESCHIKT VOOR REGELDOELEINDEN.
EUT Report 89-E-215. 1989. ISBN 90-6144-215-X

(216) Pineda de Gyvez, J.
LASER: A LAyout Sensitivity ExploreR. Report and user's manual.
EUT Report 89-E-216. 1989. ISBN 90-6144-216-8

(217) Duarte, J.L.
MINAS: An algorithm for systematic state assignment of sequential machines - computational aspects and results.
EUT Report 89-E-217. 1989. ISBN 90-6144-217-6

(218) Kamp, M.M.J.L. van de
SOFTWARE SET-UP FOR DATA PROCESSING OF DEPOLARIZATION DUE TO RAIN AND ICE CRYSTALS IN THE OLYMPUS PROJECT.
EUT Report 89-E-218. 1989. ISBN 90-6144-218-4

(219) Koster, G.J.P. and L. Stok
FROM NETWORK TO ARTWORK: Automatic schematic diagram generation.
EUT Report 89-E-219. 1989. ISBN 90-6144-219-2

(220) Willems, F.M.J.
CONVERSES FOR WRITE-UNIDIRECTIONAL MEMORIES.
EUT Report 89-E-220. 1989. ISBN 90-6144-220-6

(221) Kalasek, V.K.I. and W.M.C. van den Heuvel
L-SWITCH: A PC-program for computing transient voltages and currents during switching off three-phase inductances.
EUT Report 89-E-221. 1989. ISBN 90-6144-221-4

Eindhoven University of Technology Research Reports
Faculty of Electrical Engineering

ISSN 0167-9708
Coden: TEUEDE

(222) Jóźwiak, L.
THE FULL-DECOMPOSITION OF SEQUENTIAL MACHINES WITH THE SEPARATE REALIZATION OF THE NEXT-STATE AND OUTPUT FUNCTIONS.
EUT Report 89-E-222. 1989. ISBN 90-6144-222-2

(223) Jóźwiak, L.
THE BIT FULL-DECOMPOSITION OF SEQUENTIAL MACHINES.
EUT Report 89-E-223. 1989. ISBN 90-6144-223-0

(224) Book of abstracts of the first Benelux-Japan Workshop on Information and Communication Theory, Eindhoven, The Netherlands, 3-5 September 1989.
Ed. by Han Vinck.
EUT Report 89-E-224. 1989. ISBN 90-6144-224-9

(225) Hoeijmakers, M.J.
A POSSIBILITY TO INCORPORATE SATURATION IN THE SIMPLE, GLOBAL MODEL OF A SYNCHRONOUS MACHINE WITH RECTIFIER.
EUT Report 89-E-225. 1989. ISBN 90-6144-225-7

(226) Dahiya, R.P. and E.M. van Veldhuizen, W.R. Rutgers, L.H.Th. Rietjens
EXPERIMENTS ON INITIAL BEHAVIOUR OF CORONA GENERATED WITH ELECTRICAL PULSES SUPERIMPOSED ON DC BIAS.
EUT Report 89-E-226. 1989. ISBN 90-6144-226-5

(227) Bastings, R.H.A.
TOWARD THE DEVELOPMENT OF AN INTELLIGENT ALARM SYSTEM IN ANESTHESIA.
EUT Report 89-E-227. 1989. ISBN 90-6144-227-3

(228) Hekker, J.J.
COMPUTER ANIMATED GRAPHICS AS A TEACHING TOOL FOR THE ANESTHESIA MACHINE SIMULATOR.
EUT Report 89-E-228. 1989. ISBN 90-6144-228-1

(229) Oostrom, J.H.M. van
INTELLIGENT ALARMS IN ANESTHESIA: An implementation.
EUT Report 89-E-229. 1989. ISBN 90-6144-229-X